UNCLASSIFIED

AD NUMBER

ADC041417

CLASSIFICATION CHANGES

TO: unclassified

FROM: confidential

LIMITATION CHANGES

TO:

Approved for public release, distribution unlimited

FROM:

Distribution limited to DoD and DoD contractors only; Specific Authority; 22 Apr 87. Other requests must be referred to Director, Defense Nuclear Agency, Washington, DC 20305-1000.

AUTHORITY

DSWA ltr., 13 Apr 1998; Same

THIS PAGE IS UNCLASSIFIED

Formerly
RESTRICTED DATA
ATOMIC ENERGY ACT 1954

CONFIDENTIAL

DTIC FILE COPY

LD

DNA-5826F-SUP

AD-C041 417

DYNAMIC PRESSURE IMPULSE FOR NEAR-IDEAL AND NON-IDEAL BLAST WAVES (U)

Height of Burst Charts (U)
Supplement to DNA 5826 (U)

E. J. Bryant
F. J. Allen
Kaman Tempo
P. O. Drawer QQ
Santa Barbara, CA 93102

31 December 1983

Technical Report

CONTRACT No. DNA 001-82-C-0287

Distribution authorized to the Department of Defense and U[illegible] DoD contractors only; Specific Authority (Public Law 79-585), 22 April 1987. Other requests shall be referred to Director, Defense Nuclear Agency, Washington, DC 20305-1000.

THIS WORK WAS SPONSORED BY THE DEFENSE NUCLEAR AGENCY UNDER RDT&E RMSS CODE B344082466 Y99QAXSG00039 H2590D.

Prepared for
Director
DEFENSE NUCLEAR AGENCY
Washington, DC 20305-1000

CLASSIFIED BY DD Form 254, 15 June 1982, Contract No. DNA 001-82-C-0287, and CG-W-4, Rev. 1, "Joint DOE/DoD Nuclear Weapon Classification Guide" August 1982 (SRD(N)).

FORMERLY RESTRICTED DATA
Unauthorized disclosure subject to administrative and criminal sanctions. Handle as Restricted Data in foreign dissemination. Section 144.b, Atomic Energy Act, 1954.

CONFIDENTIAL

87 8 25 521

DISTRIBUTION LIST UPDATE

This mailer is provided to enable DNA to maintain current distribution lists for reports. We would appreciate your providing the requested information.

- ☐ Add the individual listed to your distribution list.
- ☐ Delete the cited organization/individual.
- ☐ Change of address.

NAME: ______________________________

ORGANIZATION: ______________________________

OLD ADDRESS	CURRENT ADDRESS

TELEPHONE NUMBER: (   ) ______________________________

SUBJECT AREA(s) OF INTEREST:

____

____

____

DNA OR OTHER GOVERNMENT CONTRACT NUMBER: ______________________________

CERTIFICATION OF NEED-TO-KNOW BY GOVERNMENT SPONSOR (if other than DNA):

SPONSORING ORGANIZATION: ______________________________

CONTRACTING OFFICER OR REPRESENTATIVE: ______________________________

SIGNATURE: ______________________________

CUT HERE AND RETURN

Director
Defense Nuclear Agency
ATTN: [redacted] TITL
Washington, DC 20305-1000

Director
Defense Nuclear Agency
ATTN: [redacted] TITL
Washington, DC 20305-1000

Formerly
RESTRICTED DATA
ATOMIC ENERGY ACT 1954

CONFIDENTIAL

(This page is unclassified)

UNCLASSIFIED
SECURITY CLASSIFICATION OF THIS PAGE

AD

REPORT DOCUMENTATION PAGE

1a. REPORT SECURITY CLASSIFICATION: CONFIDENTIAL	1b. RESTRICTIVE MARKINGS: FORMERLY RESTRICTED DATA
2a. SECURITY CLASSIFICATION AUTHORITY: DD Form 254, 15 June 1982, Contract No.	3. DISTRIBUTION/AVAILABILITY OF REPORT: Distribution authorized to the Department of Defense and [redacted]..DoD contractors only;
2b. DECLASSIFICATION/DOWNGRADING SCHEDULE: N/A since Formerly Restricted Data	
4. PERFORMING ORGANIZATION REPORT NUMBER(S): KT-83-032	5. MONITORING ORGANIZATION REPORT NUMBER(S): DNA-5826F-SUP PL
6a. NAME OF PERFORMING ORGANIZATION: Kaman Tempo; 6b. OFFICE SYMBOL (If applicable)	7a. NAME OF MONITORING ORGANIZATION: Director, Defense Nuclear Agency
6c. ADDRESS (City, State, and ZIP Code): P.O. Drawer QQ, Santa Barbara, CA 93102	7b. ADDRESS (City, State, and ZIP Code): Washington, DC 20305-1000
8a. NAME OF FUNDING/SPONSORING ORGANIZATION; 8b. OFFICE SYMBOL (If applicable): SPSS/Ullrich	9. PROCUREMENT INSTRUMENT IDENTIFICATION NUMBER: DNA 001-82-C-0287
8c. ADDRESS (City, State, and ZIP Code)	10. SOURCE OF FUNDING NUMBERS: PROGRAM ELEMENT NO. 62715H; PROJECT NO. Y99QAXS; TASK NO. G; WORK UNIT ACCESSION NO. DH006189

11. TITLE (Include Security Classification)
DYNAMIC PRESSURE IMPULSE FOR NEAR-IDEAL AND NON-IDEAL BLAST WAVES (U)
Height of Burst Charts (U) Supplement to DNA-5826 (U)

12. PERSONAL AUTHOR(S)
Bryant, E. J. and Allen, F. J.

13a. TYPE OF REPORT	13b. TIME COVERED	14. DATE OF REPORT (Year, Month, Day)	15. PAGE COUNT
Technical	FROM 820830 TO 831130	831231	59

16. SUPPLEMENTARY NOTATION
This work was sponsored by the Defense Nuclear Agency under RDT&E RMSS Code B344082466 Y99QAXSG00039 H2590D.

17. COSATI CODES FIELD	GROUP	SUB-GROUP
18	3	
19	9	

18. SUBJECT TERMS (Continue on reverse if necessary and identify by block number)
Nuclear Weapons Effects; Airblast (nuclear); Precursor (nuclear); Dynamic Pressure Impulse; Height of Burst; Sachs Scaling

19. ABSTRACT (Continue on reverse if necessary and identify by block number)

Blast wave data for all past field tests have been reviewed. Some previously unused gage data of sufficiently good quality for determining dynamic pressure impulse have been found and the data reduced. Dynamic pressure impulse has been inferred from tank displacement data (as was done previously using truck displacement data, Reference 1) using the curve of dynamic pressure impulse versus displacement as a calibration curve (with the tank playing the role of a gage). This allowed extension of dynamic pressure impulse results to higher values than previously available and also provided data points at additional scaled burst heights. Following this, Height of Burst Charts, i.e., iso-scaled dynamic pressure impulse contours in the scaled height of burst -- scaled ground range plane, were constructed using the totality of the useable dynamic pressure impulse data. The charts, Figures 11 and 12, are for two cases: Near-Ideal -- Lightly/Moderate Dust and Near-Ideal -- Moderate/Heavy Dust. The former is the better determined of the two. It is believed that these charts are the most accurate obtainable from the totality

20. DISTRIBUTION/AVAILABILITY OF ABSTRACT: ☐ UNCLASSIFIED/UNLIMITED ☒ SAME AS RPT. ☐ DTIC USERS	21. ABSTRACT SECURITY CLASSIFICATION: Unclassified
22a. NAME OF RESPONSIBLE INDIVIDUAL: Sandra E. Young	22b. TELEPHONE (Include Area Code): (202) 325-7042; 22c. OFFICE SYMBOL: DNA/CSTI

DD FORM 1473, 84 MAR — 83 APR edition may be used until exhausted. All other editions are obsolete.

SECURITY CLASSIFICATION OF THIS PAGE

(This page is unclassified)

CONFIDENTIAL

FORMERLY RESTRICTED DATA
Unauthorized disclosure subject to administrative and criminal sanctions. Handle as Restricted Data in foreign dissemination. Section 144.b, Atomic Energy Act, 1954.

2a. SECURITY CLASSIFICATION AUTHORITY (Continued)

DNA 001-82-C-0287 and CG-W-4, Rev 1, "Joint DOE/DoD Nuclear Weapon Classification Guide," August 1982 (SRD(N)).

3. DISTRIBUTION/AVAILABILITY OF REPORT (Continued)

Specific Authority (Public Law 79-585), 22 April 1987. Other requests shall be referred to Director, Defense Nuclear Agency, Washington, DC 20305-1000.

18. SUBJECT TERMS (Continued)

Light Dust Blast Wave
Heavy Dust Blast Wave

19. ABSTRACT (Continued)

of all existent blast wave measurements. These charts supersede the Height of Burst Charts in Reference 1.

(This page is unclassified) CONFIDENTIAL

SUPPLEMENT TO
DYNAMIC PRESSURE IMPULSE INVESTIGATIONS

PREFACE
(This Preface is Unclassified.)

We wish to thank Mrs. Jeanne Rosser for her careful attention to the many details of tabulation, curve plotting and computational checking involved in the preparation of this report. We wish to thank Mr. John Keefer, BRL, for providing BRL unpublished pressure-time records for several nuclear events; these data proved quite useful.

This page is UNCLASSIFIED.

CONFIDENTIAL

TABLE OF CONTENTS
(This Table of Contents is Unclassified)

LIST OF ILLUSTRATIONS
(This List of Illustrations is Unclassified)

LIST OF TABLES
(This List of Tables is Unclassified)

GENERAL NOMENCLATURE

I_q = dynamic pressure impulse

D = displacement

R = ground range

x = scaled ground range

HOB = height of burst

S_d, S_i, S_p, S_t = scaling factors

$$S_d = \left(\frac{P_o}{14.7}\right)^{1/3} \frac{1}{W^{1/3}}$$

$$S_i = \left(\frac{T_o(^\circ C) + 273}{288}\right)^{1/2} \left(\frac{14.7}{P_o}\right)^{2/3} \frac{1}{W^{1/3}}$$

$$S_p = \frac{14.7}{P_o}$$

$$S_t = \left(\frac{T_o(^\circ C) + 273}{288}\right)^{1/2} \left(\frac{P_o}{14.7}\right)^{1/3} \left(\frac{1}{W}\right)^{1/3}$$

P_o = ambient pressure (lbs/sq in)

T_o = ambient temperature (degrees C)

W = weapon yield (KT)

a_0, a_1, a_2, b, ℓ, m, A, B = constants in least squares fits

x,y - independent and dependent variables in least squares fits

σ = standard deviation

σ^2 = variance

N = number of data points

r = correlation coefficient

R = multiple linear correlation coefficient

GENERAL NOMENCLATURE (Continued)

r^2, R^2 = coefficient of determination

S = sum of squares of deviations of data points from fitted curve

S' = sum of squares of fractional (relative) deviations of data points from fitted curve

$\sigma' = \left(\frac{S'}{N - \text{number of regression coefficients}}\right)^{1/2}$ = standard deviation of fractional error

$E = \left(\frac{S'}{N}\right)^{1/2} \times 100$ = root mean square percent error

SO = side on

FO = face on

RO = rear on

See Appendix, "The Least Squares Procedures", for definitions/defining equations of the following specific examples of the above general quantities: σ, σ^2; r, R, r^2, R^2; $S_{\ell n\ I_q}$, $S_{\ell n\ S_iI_q}$, $S_{\ell n\ D}$; S'_{I_q}, $S'_{S_iI_q}$, S'_D; $\sigma_{\ell n\ I_q,C}$, $\sigma_{\ell n\ S_iI_q,C}$, $\sigma_{\ell n\ D,C}$; $\sigma'_{I_q,C}$, $\sigma'_{S_iI_q,C}$, $\sigma'_{D,C}$; E_{I_q}, $E_{S_iI_q}$, E_D; σ_ℓ, σ_m.

SECTION 1
(This Section is Unclassified)

INTRODUCTION

The objective was to construct improved height of burst contours for dynamic pressure impulse. In particular, we wished to extend the set of contours previously generated (Reference 1) to higher values of dynamic pressure impulse and to obtain data points along the contours at additional scaled burst heights, i.e., to better determine the contour shapes. To do this we analyzed all of the data available. This includes dynamic pressure-time waveforms for shots not used in Reference 1 (because no trucks were exposed on these shots): TEAPOT Hornet-5, Post-11, and Zucchini-14; PLUMBBOB Franklin-2, Wilson-4, Hood-6, Kepler-9, and Owens-10. It also includes data for shots in which tanks and howitzers were exposed but no dynamic pressure measurements were made: GREENHOUSE Easy-2; TUMBLER-SNAPPER Fox-6 and How-7; UPSHOT-KNOTHOLE Annie-1*, Nancy-2, Badger-5, and Simon-7.

* There was one dynamic pressure measurement on this shot.

SECTION 2
(This Section is Unclassified)

ANALYSIS OF BLAST MEASUREMENTS

2.1 Measurements For Events Not Previously Considered.

We consider first the shots not previously considered for which some dynamic pressure measurements were available. Some of the waveforms were not very good owing to noise (mixed inextricably with real physical irregularities), baseline movement, or gage record cutoff. However, many of the waveforms were found useable, being a quality similar to, or not significantly inferior to, those used in Reference 1. General information on all of the nuclear tests of concern in this report is given in Table 1. Dynamic pressure impulse, scaled and unscaled, is given in Table 2 for each Operation/Event, scaled height of burst, and ground range for which we have obtained results. Also given in Table 2 is the manner in which we obtained the values of dynamic pressure impulse.

We discuss the data for the shots in the order listed in Section 1.

TEAPOT, Hornet-5. As indicated in Table 1 we used BRL gage data.* There were two gage results at each of the three ground ranges. In two instances the two results are in good agreement. At the closest-in range, 256 meters, the two gages differ by about a factor of two but one of the two appears to be correct, the other badly in error. We used the average of the two results for the 329 and 460 metre ranges, and the apparently correct results for the 256 metre ground range.

TEAPOT, Post-11. For this shot dynamic pressure waveforms are available in Reference 2. We used a planimeter to obtain the area under each curve and then used the data reduction procedure described in detail in Reference 1. A detailed discussion of accuracy of this procedure is also given in Reference 1. For this shot waveforms are given at four ground ranges in Reference 2. The waveforms are not good but are of sufficient quality to be useful. As indicated in Table 2 we used the average of BRL's result and our result for the two ground ranges at which BRL provided results. Our results and BRL's results agreed to within about 3% which is quite good; (the two results are based on the same gage data but the data reduction procedures are independent; we have analyzed errors inherent in data reduction in Reference 1, and, in many instances, errors can be quite large).

For the two ground ranges at which BRL did not reduce the data, we used the result of our own data reduction process.

TEAPOT, Zucchini-14. For this shot we averaged our result with the result of BRL's data reduction process for the three listed ground ranges.

---

* BRL gage data used in this report are published in DNA-TR-85-161. Furnished by Mr. J. Keefer, BRL.

In each case the difference was between 3 and 5%. Results are based on two gages at the 610 and 700 metre ground ranges and upon one gage at the 794 metre range.

PLUMBBOB, Franklin-2. For this shot we used the BRL result for the single ground range for which there appeared to be a good measurement.

PLUMBBOB, Wilson-4. For this shot BRL also provided values of dynamic pressure impulse as listed in Table 2. (We integrated the waveform curves as a check, however.)

PLUMBBOB, Hood-6. Of the 6 ranges at which there were gage results the data appeared to be valid at 4 locations. There were two gages at each of these locations. We used the BRL results as listed in Table 2 (again after an integration check).

PLUMBBOB, Kepler-9. In this case waveforms obtained at three ground ranges were quite poor. In one case there was a large disparity between two BRL gage results (almost a factor of 4); in a second case there was almost a factor of 2 difference between our gage-reduced result and BRL's result. At the third ground range, 762 metres, the waveform was somewhat better. The percent difference between our result and BRL's result was rather large, about 20%; in Table 2 we list the average of the two results. We discarded the results at the other two ground ranges.

PLUMBBOB, Owens-10. For this shot we again used the average of our gage-reduced result and the BRL result at two of the three ground ranges, 305 and 518 metres. At the 305 metre range the results are in reasonably good agreement (within 9%); at the 518 metre range the two results differ by a factor of 1.4 but the waveforms are quite poor. At the 457 metre range our value of dynamic pressure impulse was exactly equal to BRL's value of scaled dynamic pressure impulse; the BRL value appeared anomalous on a data plot, probably as a result of failure to scale the value obtained. In this case we used our gage-reduced result.

2.2 Analysis of Tank Data.

We next consider the set of shots listed in Section 1 on which tanks were exposed but there were no dynamic pressure measurements. Our rationale here is based on a finding we have discussed in detail in Reference 1: the displacement which a vehicle exposed to a blast wave suffers can be used as a measure of the dynamic pressure impulse it receives. That is, the vehicle can serve as a gage for dynamic pressure impulse if we are able to "calibrate" this "gage". The calibration is the curve of dynamic pressure impulse versus displacement. (We are ignoring low yield devices where diffraction effects play a role.) We have analyzed the procedure and results for 1/4 ton and 2½ ton trucks in considerable detail in Reference 1.

We would not be able to use the procedure for tanks if we had no dynamic pressure impulse data for the ground ranges at which tanks were exposed. That is, we would have no way of obtaining the necessary calibration curve. Fortunately, we have the necessary dynamic pressure impulse data. It is supplied

by information from TEAPOT, Met-12 and Apple II-13 and from UPSHOT-KNOTHOLE, Annie-1 and Grable-10. The data for the pair of UPSHOT-KNOTHOLE events are gage data supplied by BRL; for Grable-10 we also have results based on both gage and (truck) displacement from Reference 1, but at larger values of ground range than those at which tanks were exposed. The BRL data and the Reference 1 data are very compatible, i.e., very well represented by a single curve of scaled dynamic pressure impulse versus scaled ground range (as shown in Figure 7, to be discussed later). The results are listed in Table 2.

For Met-12 we have the results from Reference 1, listed in Table 2, based on both gage and (truck) displacement data. (There is a considerably larger body of truck displacement data than of tank displacement data so that the dynamic pressure impulse - displacement curve, i.e., the calibration curve, is better determined for trucks.)

For Apple II-13 the results listed in Table 2 are taken only partly from Reference 1. In this instance, values of dynamic pressure impulse at the 518 and 625 metre ranges listed in Reference 1 (based only upon gage data) have been averaged with BRL gage results, i.e., the two results given equal weight. At the 625 metre range this makes a negligible difference while at the 518 metre range the value of dynamic pressure impulse listed in Reference 1 differs from that of Table 2 by about 16%. Finally at the 808 metre range the result listed in Table 2 differs from that listed in Reference 1; the latter is in error as a check of our (previous) data reduction reveals.

2.2.1 Dynamic Pressure Impulse Versus Displacement For Tanks.

We plotted dynamic pressure impulse versus displacement for the tanks exposed on events Met-12, Apple II-13, Annie-1 and Grable-10. This provides a total of 14 data points* listed in Table 3 along with the tank displacement data for other shots.

There are several variables which cause deviations of the data relative to a smooth curve through the points: (1) vehicle orientation with respect to the bomb -- 4 data points correspond to side-on orientation, 7 to face-on orientation, 1 to rear-on orientation, 1 to face-on 45° orientation, and 1 to face-on 3/4 left orientation; (2) there are three different tanks -- M4A3, M24, and M48; (3) there are two surface conditions -- rough sand and fine sand. There obviously are not sufficient data to sort out the effects of the variables. However, when we plotted the data we found that: (1) (initial) orientation appears to make little difference, any effect being submerged in effects of the other variables; (we intuitively expect initial orientation to make less difference for tanks than for trucks); (2) any systematic deviation which could be attributed to type of vehicle could as well be attributed to inaccuracy in dynamic pressure impulse -- for example, the Met-12 points (points B, 6, and 17 in Table 3) are a little high and are

* We have not used Point 8 of Table 3, a Smoky-15 point. Placing this point on Figure 1 shows that there is clearly something wrong with it -- and what is wrong with it involves the displacement, not the dynamic pressure impulse, even though the latter involves extrapolation on Figure 6.

M48 points while the Apple II-13 points are a little low and pertain to both M48's and M24's. (In fact, if we use an average dynamic pressure impulse versus scaled ground range curve for the two shots, Met-12 and Apple II-13, these deviations disappear.)

Plots of the data and the fits obtained are shown in Figure 1.*

We used these data to infer dynamic pressure impulse from the measured displacements on events GREENHOUSE Easy-2; UPSHOT-KNOTHOLE Nancy-2, Badger-5, and Simon-7; TUMBLER-SNAPPER Fox-6 and How-7.

We have noted in Reference 1 that, despite rather wide fluctuations in displacement owing to the several variable factors mentioned, the central curve following the trend of the data points provides a rather good calibration which enables us to use a measured displacement to determine the dynamic pressure impulse to which the vehicle was subjected. Since displacements vary owing to uncontrolled factors, the inferred dynamic pressure impulses will exhibit considerable dispersion. (However, in many cases described in Reference 1, the displacement-inferred values are about as reliable as the gage-inferred values, especially when there are two or more values which can be averaged.)

The calibration curve for tanks is less well determined than that for trucks (Reference 1), there being fewer data points. Also the displacements are smaller resulting in greater errors especially from small yield. Nonetheless, when the displacement-inferred dynamic pressure impulse values are plotted versus scaled ground range (along with a few data points for which there also are gage data), we see that the curve obtained is reasonably well determined. See Figure 3.

We used an eye-drawn curve rather than a proportional fit in Figure 1 in inferring dynamic pressure impulse from measured displacements for the following reasons:

(1) point 20, very small displacement, is much less important than the other data points in application of this fit, i.e., inference of dynamic pressure impulse from measured displacement;

(2) point 21 has virtually the same displacement as the centroid so that it can be ignored in drawing a straight line through the data points; [the line must pass through the centroid:

$$\overline{\ln D} = 2.448, \ \overline{\ln I_q} = 3.768;$$

on the abscissa and ordinate scales from Figure 1 we see that both fits do pass through the point $\overline{D(\ln D)} = 11.56$, $I_q\overline{(\ln I_q)} = 43.29$; the lines do <u>not</u> pass through the point $\overline{D} = 21.85$, $\overline{I_q} = 47.95$];

* Because of the mentioned variables whose effects we cannot disentangle owing to the small amount of data, we have numbered the points on Figure 1. Corresponding numbers are listed in Table 3. By comparison one can verify that the data do not exhibit any marked effects owing to differences among the above variables.

(3) the Grable-10 points 21 and 22 are badly inconsistent with one another and points 9 and 10 are somewhat inconsistent. Thus our eye-drawn curve was a little higher than Fit 1 of Figure 1 at the small displacement end and, like Fit 1, passed through the centroid of the data points. The difference, however, is nowhere greater than a few percent. We also note from Figure 1 that a curve through the data points would do no better than a straight line and is therefore not warranted. It is quite possible, however, that if the data covered a wider range a straight line would no longer be adequate.

2.3 Discussion Of and Minor Improvements Upon Previously Used Blast Data.

Most of the dynamic pressure impulse data listed in Table 2 which we have not yet discussed is taken from Reference 1. In a few instances a value taken from Reference 1 (gage only - no vehicle displacement data available) was averaged with a BRL gage-reduced result as shown in the table. In one instance, Turk-4, ground range 595 metres, we reduced the gage data even though the gage had cut off near the end. We estimated the shape and time of pulse completion from other Turk-4 data and believe that the inaccuracy so introduced is small — not more than a few percent. Reference to Figure 3 shows why this is desirable: Turk-4 has the lowest scaled burst height for which we have gage data (except for a single Annie-1 point and except for surface burst data); its scaled burst height is only moderately greater than those of other events shown on Figure 3; the Turk-4 data are consistent with the data for the other events shown on Figure 3 and extend to a much greater value of scaled ground range. Thus the curve fit of Figure 3 is not diminished in reliability by inclusion of Turk-4 data which, however, enable its use over a much greater range in constructing height of burst charts, the object of this report.

For events Yuma-4 and Wasp Prime-9 we used our values from Reference 1, therein described as "first iteration" results; i.e., when available, truck displacement-inferred dynamic pressure impulse values were averaged with gage values in obtaining our best estimates of dynamic pressure impulse. (The manner of averaging, justification, and discussion of accuracy and reliability are considered in detail in Reference 1.) We originally considered Yuma-4 to be an ideal event, but we now believe the values achieved by averaging displacement-inferred dynamic pressure impulse values with the gage values represent an improvement over the gage values alone; the results achieved are certainly more compatible with the other data in the same scaled height of burst region. See Figure 9 (and compare with gage only data listed in Reference 1, page 115).

For event Encore-9, a near-ideal event, we use the gage results -- even though in Reference 1 we sought to improve upon these results by use of displacement-inferred dynamic pressure impulse. The reasoning used in Reference 1 was that since the data scatter on a displacement versus dynamic pressure impulse plot was just as great for ideal/near-ideal shots as for non-ideal and since the displacement-inferred dynamic pressure impulse for non-ideal shots is, on the average, as accurate and reliable as the gage values -- then averaging of displacement-inferred with gage-inferred dynamic pressure impulse should improve the values for near-ideal events just as it does for non-ideal. The points at issue are discussed in detail in Reference 1. One point, however,

is that there is a much greater variety of ideal/near-ideal shots than of non-ideal, especially regarding the range of weapon yields in the data base. When good gage data are available, these data should produce better results than can be obtained by averaging in displacement-inferred values -- owing to the effects of the several uncontrolled variables previously described. That is, while, on the average, displacement-inferred values are reliable, considerable dispersion is to be expected. Compare, for example, Figure 3; here with the exception of the Turk-4 data points and a single Annie-1 point, all of the plotted points are based entirely upon displacement-inferred values of dynamic pressure impulse. While the central curve following the general trend of the data is reasonably well determined, the data point deviations are rather large -- considerably larger than the deviations in Figures 4-10.

Near-ideal shots also have (small) real differences relative to one another. This is shown, for example, by Figure 3.13 of Reference 1 which is a plot of scaled dynamic pressure impulse versus scaled ground range. Data for the near-ideal (surface burst) shots do not completely coalesce under the scaling -- there are clearly small but real differences owing to variable factors not controlled in the experiments. In Figures 3-10 the data for the events plotted on each figure seem to coalesce quite well with respect to a single curve. In Figure 7 some deviation can be seen. In general, deviations tend to appear when data for several events are shown on a single plot, when there are several data points for each event, and where the data for several events overlap, i.e., cover the same domain of the abscissa, scaled ground range. The data in Figures 3-10 pertain to a much smaller range of weapon yields than do the surface burst data of Reference 1 (Figures 3.13 and 3.15). In general, when the data for several shots coalesce we can attach a high degree of reliability to the data.

In constructing height of burst charts in this report we used the results described and listed in Table 3. For the surface burst data we used Figure 3.13 of Reference 1.*

Finally we analyzed field data for many more shots, but found the data unusable. In some instances the waveforms were very bad; in other instances the gages were placed at elevations other than 3 feet above the ground. The effect of gage elevation is non-negligible. (Different types of gages also exhibit somewhat different responses which must be accounted for in order to achieve consistent results.)

NOTE: The BRL data used in Table 3 have not been published.

2.4 Dynamic Pressure Impulse Versus Displacement for Self-Propelled Howitzers.

Figure 2 is a plot of displacement - dynamic pressure impulse data for

* For a single (extrapolated) point on the charts for which the scaled dynamic pressure impulse is 15 kPa-sec and the scaled height of burst is zero, we also used Figure 3.15 of Reference 1 and took account of the difference between Figures 3.13 and 3.15 in this region. Figure 3.15 extends to slightly higher values of dynamic pressure impulse than does Figure 3.13 so that less extrapolation is required.

self-propelled howitzers. Here we used values of dynamic pressure impulse already described. There are only eight data points. These involve 2 vehicles, 3 orientations, 2 soil types and 7 nuclear events. Three of the data points (2 Badger-5 and 1 Simon-7) result from shots for which there were no dynamic pressure measurements. Therefore, the values we used, taken from Figure 3 and from the scaled height of burst chart, Figure 11, are actually based upon the displacement-inferred dynamic pressure impulse values for tanks.

We did not attempt to use the howitzer displacement data to infer values of dynamic pressure impulse. To do so, we should proceed in the same manner as for the tank data. Referring to Figure 2, we see that of the eight data points only five (points 31-35) could be used. No curve of any reasonable degree of reliability can be drawn based on these points.

SECTION 3
(This Section is Unclassified)

RESULTS AND CONCLUSIONS

The results described are given in Tables 2 and 3. Least squares fits are given in Tables 4 and 5. A description of the methods used in obtaining these fits and the definitions and explanations of the several measures of goodness of fit listed are given in the Appendix. The simplest measure of goodness of fit to understand is the root mean square percent error (E_D and E_{I_q}). From Table 4 we see that for the displacement - dynamic pressure impulse fits, the errors are quite large.* The error in estimating dynamic pressure impulse from given displacement is fairly large (35-40%) but tolerable and as we have seen the values obtained, on the average, are reasonable and of considerable value especially when gage data are poor or lacking. If we were, however, to attempt to infer displacement from a given dynamic pressure impulse the errors would be much larger (∿150%) -- though again the results would represent reasonable approximations to the average displacement to be expected. (The reason for the wide disparity between the errors for the two types of inference is seen to be simply due to the slope of the fitted lines on the log-log plots, Figures 1 and 2, or equivalently from the exponents in the fits listed on the Figures and in Table 4.)

The percent errors, E_{I_q}, shown, in Table 5 for the dynamic pressure impulse versus scaled ground range fits are quite modest, varying from about 4 to 25%. These errors are quite comparable to those obtained in Reference 1 for the various fits therein.

The results described are shown along with the fits, in Figures 1 - 10. These results were then used, along with the surface burst data in Reference 1 (Figure 3.13 and in one instance Figure 3.15) to construct the desired scaled dynamic pressure impulse contours as shown in Figures 11 and 12. Also shown is the locus of points separating the regular and Mach reflection regions.

We have drawn the contours to conform as accurately as possible to the plotted points while maintaining smoothness and a continuous variation in contour shape as we proceed from low to high values of scaled dynamic pressure impulse.

Figure 11 is the better and more reliable of the two charts. The curves fit the data points much better than for Figure 12. In the latter case we have not attempted to force the curves through the data points as this would lead to structure in the contour shapes which is not justified by the data.

There are various degrees of dust**, the Met-12 data corresponding to the heaviest dust case while the Apple II-13 and Bee-6 data represent more moderate

* The errors here are much larger than in Reference 1 because there are much more data for trucks (of concern in Reference 1) than for the tanks and howitzers of concern here.

** We now believe that the degree of "dustiness" is an indicator of the severity of the precursor which is related in turn to the temperature of the preshock thermal layer.

dust. This is the principal cause of the difficulty in Figure 12. However, we do not believe that separate charts for moderate dust and for heavy dust are warranted. This distinction is simply too fine considering the quality of the data.

In conforming the contours to the data points in as reasonable a manner as possible, we note that the two charts differ for the higher scaled burst heights, i.e., the comparable contours do not coincide, even though the same data are used for the two highest scaled burst heights on Figures 11 and 12. We cannot regard the contours in this region as well determined; our preference in this region is for Figure 11, because of the greater smoothness of the contours and because we believe the data at the third highest scaled burst height are better for Figure 11 than for Figure 12.

Note: In applications of Figures 11 and 12 the scaling factor S_d (see General Nomenclature) should be used rather than $W^{-1/3}$ for scaling ground range and height of burst; S_i should be used in conjunction with contours rather than $W^{-1/3}$ for instances in which ambient pressure and temperature are specified and differ significantly from the standard values of 14.7 psi (101.4 kPa) and 15°C, respectively.

SECTION 4
(This Section is Unclassified)

RECOMMENDATION

It is recommended that the Height of Burst Chart, Figure 11, be accepted as standard, i.e., as the most accurate obtainable from the totality of existent blast wave measurements. Figure 12 which includes I_q for moderate/heavy dust environments is for unique conditions. The description of these conditions was discussed in Reference 1. Thus, Figure 12 should be used only for similar conditions or be ignored.

REFERENCES

(This List of References is Unclassified)

1. E. Bryant and F. Allen, "Dynamic Pressure Impulse for Near-Ideal and Non-Ideal Blast Waves — Height of Burst Charts (U)", KT-81-014(R), 15 May 1981. Final Report, Part I, 15 Feb 1980 to 15 Apr 1981 on Contract No. DNA001-80-C-0156. (SECRET)

2. E. J. Bryant, N. H. Ethridge and J. H. Keefer, "Measurements of Air-Blast Phenomena with Self-Recording Gages, Operation Teapot - Project 1.14b", WT-1155, 16 July 1959.

3. P. G. Guest, Numerical Methods of Curve Fitting, Cambridge University Press, 1961.

4. Paul G. Hoel, Introduction to Mathematical Statistics, John Wiley and Sons, Inc., New York, 1954.

5. Irvin Guttman and S. S. Wilks, Introduction to Engineering Statistics, John Wiley and Sons, Inc., New York, 1965.

6. Ya-lun Chou, Statistical Analysis, Holt, Rinehart and Winston, New York, Second Edition, 1975.

APPENDIX A
(This Appendix is Unclassified)

THE LEAST SQUARES PROCEDURES

1. INTRODUCTION.

All of the least squares fits in this report were obtained with the TI-59 calculator using library programs supplied by Texas Instruments.

All of the fits were either of the form

$$y = mx + b \tag{1}$$

or

$$y = a_0 + a_1x_1 + a_2x_2 \tag{2}$$

where y was the natural logarithm of the desired quantity; x was either the independent (controlled) variable or its logarithm and the least squares variables x_1, x_2 involved only the special case $x_1 = x$ and $x_2 = x^2$.

The least squares equations are obtained by minimizing the sum of the squares of the deviations of the data from the curve. If the experimental points have a variable scatter for a given small range of x, weights should be applied in the procedures so that the least squares equations corresponding to Equation (1), for example, are obtained by setting the derivatives of

$$S = \Sigma W_i[y_i - (mx_i + b)]^2 \tag{3}$$

with respect to m and b equal to zero, thus obtaining two linear algebraic equations which can be solved for m and b. Here S is the weighted sum of the squares of the residuals about the fitted curve and

$$W_i = \sigma^2/\sigma_i^2$$

where σ is a constant (to be determined from the deviations of the data from the fitted curve) and σ_i^2 is a measure of the expected deviation from the true value for an observation y_i (of unit weight).

In the Texas Instruments programs $W_i = 1$. In individual cases to be discussed we will point out that the programs used are nonetheless quite adequate for our needs. This is mainly due to the fact that, in all cases, we minimized the sum of the squares of the <u>logarithm</u> of the desired function. This is equivalent to minimizing the sum of the squares of the <u>percentage</u> deviations from the curve since

$$\Delta(\ln y) = \frac{\Delta y}{y} \;. \tag{4}$$

That is, for small deviations from the curve, the fractional error $\frac{\Delta y}{y}$ is equal to $\Delta(\ell n\ y)$. For large deviations this is not exact and in our tabulation of results we show both

$$\sum_i (\ell n\ y_i - \ell n\ y_c)^2 \quad \text{and} \quad \sum_i \left(\frac{y_i - y_c}{y_c}\right)^2$$

where y_c = the value of $y(x_i)$ corresponding to the curve fit.*

The statistical analog of Equation (4) (Reference 3) is

$$\text{Var}\ (\ell n\ y) = \frac{1}{y^2}\ \text{Var}\ y \qquad (\text{Var} = \text{variance})\ . \qquad (4a)$$

Now in all of the cases the values of y covered a large range. If we consider, for example, a displacement measurement of 100 metres to be in error by 2%, the square of its deviation from the true value is 4; if we consider a displacement measurement of 1 metre to be in error by 20%, the square of its deviation from the true value is 0.04. So even though the percent errors in our data are not necessarily uniform (as best these errors are known), assuming them to be uniform is much closer to reality than any other assumption we can make. From the example just given we readily see that the coefficients in the least squares fits would be determined almost entirely by the data with large values of y if we were to minimize absolute rather than percent deviations from the fitted curves.

2. DYNAMIC PRESSURE IMPULSE VERSUS DISPLACEMENT (a) DISPLACEMENT VERSUS DYNAMIC PRESSURE IMPULSE (b)

In application of our results we need fits of the data for cases (a) and (b), i.e., with each quantity used in the role of independent (controlled) and of dependent variable.

In each subcase of this case the data are fitted very well by straight lines on log-log plots. Thus for fitting on the TI-59 calculator the fit is of the form

of the form	$y = mx + b$		(1)
with	$y = \ell n\ I_q,\ x = \ell n\ D$	for Case	(a)
and	$y = \ell n\ D,\ \ x = \ell n\ I_q$	for Case	(b)
and	$b = \ell n\ B$.		(5)

---

* In most cases we omit the subscript i denoting the ith data point; the summations are taken over the data points in all cases so that omission of the subscript i will not lead to any confusion.

Equation (1) can then also be written [for Case (a)], $I_q = BD^m$ (1a)
with a similar relation for Case (1b). However, after we have fitted Case (a) we can calculate (b) directly (without fitting it) provided we recall certain data summations from the machine memory. For Equation (1) we obtain from the TI-59 fit:

$$\text{slope} = m = \frac{\Sigma xy - \Sigma x \Sigma y/N}{\Sigma x^2 - (\Sigma x)^2/N} \quad (6)$$

$$y_{\text{intercept}} = b = \frac{\Sigma y - m\Sigma x}{N} \quad (7)$$

and the correlation coefficient, $r = m \left(\frac{\sigma_x^2}{\sigma_y^2}\right)^{1/2}$. (8)

r^2 is called the coefficient of determination. The various summations can be recalled from the machine memory. σ_x^2 and σ_y^2 are the variances of the x-array and y-array data and are given by *

$$\sigma_x^2 = \frac{1}{N} \Sigma(x_i - \bar{x})^2 \quad (9)$$

$$\sigma_y^2 = \frac{1}{N} \Sigma(y_i - \bar{y})^2 \quad (10)$$

with $\bar{x} = \frac{1}{N} \Sigma x$ (11)

and $\bar{y} = \frac{1}{N} \Sigma y$. (12)

N is the number of data points.

Equations (6) to (8) are not symmetrical in x and y and the algebraic inverse of the least squares fit $I_q = BD^m$ (1a)

is $D = \left(\frac{1}{B}\right)^{1/m} I_q^{1/m}$ but this is not a least squares fit to the data with the roles of I_q and D reversed.

However, manipulation of Equations (6) to (10) leads to the equation

$$r = \left[\Sigma xy - \frac{1}{N} \Sigma x \Sigma y\right] \left(\left[\Sigma x^2 - \frac{1}{N} (\Sigma x)^2\right]\left[\Sigma y^2 - \frac{1}{N} (\Sigma y)^2\right]\right)^{-1/2} \quad (8a)$$

which is symmetrical in x and y, i.e., unchan[illegible] when x and y are interchanged.

* Bar over a quantity indicates an average value.

Thus, if we have obtained the least squares fit $I_q = BD^m$ we know that the correlation ratio r has the same value with the roles of I_q and D reversed. It can be shown (by taking the origin at the data centroid), (References 3 and 4), that the least squares fits

$$I_q = BD^m \tag{1a}$$

$$D = AI_q^{\ell} \tag{1b}$$

have values of ℓ and m which satisfy $\ell m = r^2$. (13)

Thus, having determined m (and r) in the least squares fit to case 1a we obtain ℓ in the least squares fit to Case (1b) from Equation (13). The constant A in Equation 1b is then determined by the fact that both least squares fits (1a) and (1b) pass through the centroid of the data distribution. (Compare Reference 5.) Thus, from Equation (1b) we have

$$\ell n\ D = \ell n\ A + \ell\ \ell n\ I_q \tag{1b}$$

and in particular

$$\overline{\ell n\ D} = \ell n\ A + \ell\ \overline{\ell n\ I_q} \tag{14}$$

where from Equations (11) and (12)

$$\overline{\ell n\ D} = \frac{1}{N} \Sigma(\ell n\ D) \tag{15}$$

$$\overline{\ell n\ I_q} = \frac{1}{N} \Sigma(\ell n\ I_q)$$

and these values are available from the machine memory after running case (1a). Thus from Equation (14) we determine ℓn A, hence A and the least squares fit to case (1b) is fully determined.

Having obtained the least squares fits, the coefficient of determination provides a measure of the goodness of fit. By manipulation of Equation (3), with $W_i = 1$, and Equations (6) through (12) it can be shown that

$$1 - r^2 = \frac{S}{N\sigma_y^2} \quad . \tag{16}$$

In this report we are concerned only with positive correlation, so that the nearer r is to +1, the smaller is S, the sum of the squares of the deviations from the fitted curve, and hence the better the fit to the data. The expression for $1 - r^2$ can also be put in the form

$$1 - r^2 = \frac{\Sigma(y - y_c)^2}{\Sigma(y - \bar{y})^2} \tag{17}$$

thus expressing $1 - r^2$ as a ratio of the sum of the squares of the deviations from the curve to the sum of the squares of the deviations from the mean (of the data). The denominator may be regarded as a normalizing factor. It is independent of the functional form used for the fitting function. Without such a denominator $1 - r^2$ would tend to increase with the number of data points — even if the data were excellent.

Now letting $S_{\ell n\ I_q}$ and $S_{\ell n\ D}$ be the sum of the squares of the deviations from the fitted curve when $\ell n\ I_q$ and $\ell n\ D$, in turn, play the role of dependent variable, we have from Equation (16)

$$(1 - r^2) = \frac{S_{\ell n\ I_q}}{N\sigma^2_{\ell n\ I_q}} = \frac{S_{\ell n\ D}}{N\sigma^2_{\ell n\ D}} \quad . \tag{18}$$

Here
$$\sigma^2_{\ell n\ I_q} = \frac{1}{N}\left[\Sigma(\ell n\ I_q)^2 - \frac{1}{N}(\Sigma \ell n\ I_q)^2\right]$$
$$\sigma^2_{\ell n\ D} = \frac{1}{N}\left[\Sigma(\ell n\ D)^2 - \frac{1}{N}(\Sigma \ell n\ D)^2\right] \tag{19}$$

in accord with Equations (9) through (12). Since we have seen that r is unchanged when the roles of D and I_q are reversed, Equation (18) shows that the sums of the squares of the deviations from the curves are not the same for the two corresponding least squares fits (to the same data) but that

$$\frac{S_{\ell n\ I_q}}{S_{\ell n\ D}} = \frac{\sigma^2_{\ell n\ I_q}}{\sigma^2_{\ell n\ D}} \quad . \tag{20}$$

In all cases treated in this report we found $S_{\ell n\ I_q}$ to be considerably less than $S_{\ell n\ D}$.

In an application to be made of the results of this case we wish to know the standard deviation of the value of the slope of the curve as well as the standard deviation of our observation. We use the following notation with the subscript c referring to the curve fit in each instance:

$\sigma^2_{\ell n\, I_q,C}$ = variance of an observation of $\ell n\, I_q$ relative to the curve; (note that we have assumed the variance of the percent error to be independent of the abscissa value)

σ^2_ℓ, σ^2_m = variance of slopes of curve fits.

Then it can be shown that (Reference 6)

$$\sigma^2_{\ell n\, I_q,C} = S_{\ell n\, I_q} \Big/ N-2^{*}$$

$$\sigma^2_{\ell n\, D,C} = S_{\ell n\, D} \Big/ N-2 \qquad (21)$$

$$\sigma^2_\ell = \frac{S_{\ell n\, D} \Big/ N-2}{N\sigma^2_{\ell n\, I_q}} = \frac{1-r^2}{N-2}\,\frac{\sigma^2_{\ell n\, D}}{\sigma^2_{\ell n\, I_q}}$$

$$\sigma^2_m = \frac{S_{\ell n\, I_q} \Big/ N-2}{N\sigma^2_{\ell n\, D}} = \frac{1-r^2}{N-2}\,\frac{\sigma^2_{\ell n\, I_q}}{\sigma^2_{\ell n\, D}} \qquad (22)$$

Using Equation(8) twice, first with D, I_q being independent and dependent variable and then with their roles reversed, we also see that

$$\frac{\sigma_\ell}{\sigma_m} = \frac{\ell}{m} \quad . \qquad (23)$$

In the tabular results for the Displacement - Dynamic Pressure Impulse data curve fits, we list for each subcase the quantities N, $S_{\ell n\, I_q}$, $\sigma_{\ell n\, I_q,C}$, $S_{\ell n\, D}$, $\sigma_{\ell n\, D,C}$, ℓ, m, σ_ℓ, σ_m in addition to r and the fitting functions.

To gain further insight into the reliability of the data fits we have also tabulated the following additional quantities defined as follows:

* Here there are N-2 degrees of freedom; the two degrees of freedom lost correspond to the number of regression coefficients (two).

$$S'_D = \Sigma\left(\frac{D - D_C}{D_C}\right)^2$$

$$S'_{I_q} = \Sigma\left(\frac{I_q - I_{qC}}{I_{qC}}\right)^2 \qquad (24)$$

$$\sigma'_{D,C} = \left(\frac{S'_D}{N-2}\right)^{1/2}$$

$$\sigma'_{I_q,C} = \left(\frac{S'_{I_q}}{N-2}\right)^{1/2} \qquad (25)$$

and finally the root mean square percent error which is

$$E_D = (S'_D/N)^{1/2} \times 100\%$$

$$E_{I_q} = (S'_{I_q}/N)^{1/2} \times 100\% \qquad (26)$$

The σ' quantities, Equation (25), are standard deviations of the fractional error (percent error apart from a factor of 100). Thus when the number of data points N is fairly large (large enough so that the fit is fairly reliable) the values of $\sigma'_{D,C}$, $\sigma'_{I_q,C}$ are almost the same as the values of E_D and E_{I_q}, respectively, (aside from the factor of 100 expressing the latter quantities in percent).

The reason we have chosen to list these additional quantities, in this and in other data fits to be discussed shortly, is that in many cases the data scatter is rather large (irrespective of the functional form selected for fitting the data). This means that a deviation $\Delta \ln y$ in $\ln y$ for a given data point may differ considerably from $\Delta y/y$. To illustrate, suppose the curve fit and data point values of a displacement are 10 metres and 6 metres. The contribution of this point to the sum of the squares of the deviations of $\ln D$ is then $(\ln 10 - \ln 6)^2 = 0.261$ (irrespective of which value is the curve fit value and which is the data point value).

The contribution to S'_D is

$$\left(\frac{10-6}{10}\right)^2 = 0.160$$

if the curve fit value is 10 and the data point value is 6; if, however, the

curve fit value is 6 and the data point value is 10, the contribution to S'_D is

$$\left(\frac{10-6}{6}\right)^2 = 0.444.$$

Since the least squares curve tends to pass through the data region with a fairly uniform distribution of points on either side, on the average the curve fit will be below the data point about as often as above it. Averaging the above results yields $\frac{0.160 + 0.444}{2} = 0.302$ which is to be compared with the value 0.261 for the logarithmic deviation. Had we chosen the values 10 and 9.8 instead of 10 and 6, the two compared numbers would be virtually identical.

It is inherent in the nature of the data we are dealing with in this report that there is large data scatter while the number of data points is quite small. We found (Reference 1), using the same least square procedures described herein, that, when the scatter of the data is small, S'_D is fairly close in value to $S_{\ell n\,D}$ and similarly S'_{I_q} is fairly close to $S_{\ell n\,I_q}$. Usually $S_{\ell n\,D} < S'_D$ and $S_{\ell n\,I_q} < S'_{I_q}$. The situation is sometimes reversed, however, usually because one or two data points with large deviations from the curve fit are below the curve. Conversely, for a case in which one or two data points are far <u>above</u> the curve it can happen that $S'_y \gg S_{\ell n\,y}$ since there is no limit to the contribution such a point can make to S'_y, y here indicating any quantity whose ℓn has been fitted. (For a data point <u>below</u> the curve fit the maximum contribution to S'_y is

$$\left(\frac{y-y_c}{y_c}\right)^2 = \left(\frac{0-y_c}{y_c}\right)^2 = 1 \quad .)$$

The results shown in Table 4 are consistent with these statements taken from Reference 1. [The large effect which a single data point can have may be seen by calculating $\left(\frac{D-D_c}{D_c}\right)^2$ for point 31 of Figure 2. The value, 18.52, is almost as large as S'_D (= 19.06) for the 8 data points of Figure 2.]

Finally, quantities such as $\sigma'_{I_q,C}$ and E_{I_q} are directly associated with the plotted data and are easily visualized. Since they pertain to fractional or percent errors they apply equally well at all points along the curve fit (although the curve fit has greater predictive accuracy in the vicinity of the data centroid than toward the ends of the data range). On the other

hand $\sigma_{\ell n\ I_q}$ refers to the natural logarithm of the plotted data (ordinate) and the latter may be quite small or large (or even negative), so that while $\sigma_{\ell n\ I_q}$ is a standard measure of the data scatter with respect to the fitted curve, it is not as simple to interpret as are the additional quantities which we have tabulated.

In sum, the tabulated measures of goodness of fit provide some insight into the assessment of the reliability and utility of the data and the curve fits and help with the interpretation of results.

The quantities described here are also tabulated for various curve fits of data other than displacement-dynamic pressure impulse data. We discuss the least squares treatment of the remaining data in the following section.

3. ADDITIONAL LEAST SQUARES FITS.

Scaled Dynamic Pressure Impulse versus Scaled Ground Range:

The fitted curve is given by

$$y = a_0 + a_1 x + a_2 x^2 \tag{27}$$

where x = scaled ground range, $y = \ell n\ S_i I_q$.

In running this case on the TI-59 calculator we feed in the natural logarithm of each data point. Again, the machine generates a fit and all of the relevant summations over the data are available from the machine memory. For this type of fit (trivariate), however, the machine provides a quantity R^2 rather than r as a measure of the goodness of fit. R is the multiple linear correlation coefficient between y and the other least squares variables $x_1 = x$ and $x_2 = x^2$; R^2 is called the coefficient of determination (see Reference 6) and is given by

$$R^2 = \frac{r_{y1}^2 + r_{y2}^2 - 2r_{12}\ r_{y1}\ r_{y2}}{1 - r_{12}^2} \quad . \tag{28}$$

The subscripts 1 and 2 refer to x_1 and x_2; r_{y1}, r_{y2}, and r_{12} are given by equations analogous to Equation (8a).

$$r_{y1} = [\Sigma xy - \frac{\Sigma x \Sigma y}{N}] \left([\Sigma x^2 - \frac{(\Sigma x)^2}{N}][\Sigma y^2 - \frac{(\Sigma y)^2}{N}] \right)^{-1/2} \tag{29}$$

$$r_{y2} = [\Sigma x^2 y - \frac{\Sigma x^2 \Sigma y}{N}] \left([\Sigma x^4 - \frac{(\Sigma x^2)^2}{N}][\Sigma y^2 - \frac{(\Sigma y)^2}{N}] \right)^{-1/2}$$

$$r_{12} = [\Sigma x^3 - \frac{\Sigma x \Sigma x^2}{N}] \left([\Sigma x^2 - \frac{(\Sigma x)^2}{N}][\Sigma x^4 - \frac{(\Sigma x^2)^2}{N}] \right)^{-1/2} \tag{29}$$

(The superficial lack of symmetry between r_{y1} and r_{y2} results from the fact that the least squares variables x_1 and x_2 as used here are x and x^2, respectively.) The quantities r_{y1}, r_{y2}, and r_{12} are the coefficients of correlation (also called simple correlation or zero-order coefficients) between y and x_1, y and x_2, and x_1 and x_2, respectively. The important point here is that

$$(1 - R^2) = \frac{\Sigma(y-y_c)^2}{\Sigma(y-\bar{y})^2} \tag{17a}$$

so that R^2 provides a measure of the goodness of fit precisely similar to that provided by r^2 in the previous discussion: R^2 is a measure of the closeness of fit of the regression plane (in $\ell n\, y$, x_1, x_2 space)* to the data points.

There are two further changes: replacement of N-2 by N-3 in Equations (21) and (25) and replacement of I_q by $S_i I_q$

$$\sigma^2_{\ell n\, S_i I_q, C} = S_{\ell n\, S_i I_q} / N-3$$

$$\sigma^2_{\ell n\, D, C} = S_{\ell n\, D} / N-3 \tag{21a}$$

and

$$\sigma'_{D,C} = (S'_D / N-3)^{1/2}$$

$$\sigma'_{S_i I_q, C} = (S'_{S_i I_q} / N-3)^{1/2} \tag{25a}$$

Referring to the results listed in Table 5 we see that usually $S_{\ell n\, S_i I_q} < S'_{S_i I_q}$ (and in fact this relation holds for all of the cases where the number of data points ≥ 11). The two values are usually quite close, however, as might be expected, since the data dispersion is fairly modest.

---

* $x_1 = x =$ scaled ground range $\quad x_2 = x^2$

TABLE 1. (U) GENERAL INFORMATION -- NUCLEAR TESTS

CONFIDENTIAL - FORMERL: RESTRICTED DATA

OPERATION/EVENT	YIELD (KT)	HOB (m)	SCALED HOB (m)	S_p	S_d	S_t	S_i
				SCALING FACTORS			
Greenhouse, Easy-2	46.7	91.4	25.4	1.003	0.277	0.283	0.284
Tumbler-Snapper, Fox-6	11.1	91.4	38.8	1.182	0.424	0.427	0.505
How-7	14.6	91.4	35.4	1.176	0.388	0.387	0.455
Upshot-Knothole, Annie-1	16.2	91.4	34.4	1.158	0.376	0.368	0.426
Nancy-2	24.5	91.4	29.9	1.165	0.327	0.324	0.378
Badger-5	23.0	91.4	30.5	1.176	0.333	0.329	0.387
Simon-7	43.4	91.4	24.7	1.165	0.271	0.269	0.313
Encore-9	26.0	738.5	240	1.126	0.324	0.325	0.366
Grable-10	14.9	159.7	62.4	1.124	0.391	0.391	0.440
Teapot, Moth-2	2.39	91.4	65.0	1.163	0.711	0.687	0.799
Turk-4	43.0	152.4	41.1	1.187	0.271	0.265	0.315
Hornet-5	3.61	91.4	56.9	1.150	0.622	0.605	0.696
Bee-6	7.76	152.4	73.3	1.163	0.481	0.467	0.543
Apple I-8	14.2	152.4	59.2	1.188	0.392	0.387	0.460
Wasp Prime-9	3.16	225.2	145	1.193	0.642	0.640	0.763
Post-11	1.45	91.46	76.6	1.174	0.837	0.824	0.967
Met-12	22.0	121.9	41.8	1.115	0.344	0.350	0.390
Apple II-13	28.5	152.4	47.2	1.184	0.311	0.310	0.367
Zucchini-14	28.2	152.4	47.3	1.190	0.310	0.302	0.359
Redwing, Yuma-4*	0.185	62.4	109	1.012	1.748	1.785	1.806
Plumbbob, Franklin-2	0.138	93.0	171	1.165	1.839	1.858	2.164
Wilson-4	10.3	152.4	66.9	1.149	0.439	0.440	0.506
Hood-6	74.1	457.2	103.6	1.158	0.227	0.227	0.263
Kepler-9	10.3	152.4	66.5	1.171	0.436	0.438	0.513
Owens-10	9.6	152.4	68.3	1.163	0.448	0.448	0.[illegible]21
Smoky-15	43.71	213.4	57.3	1.184	0.266	0.274	0.324

* This event and yield in combination is CONFIDENTIAL-FORMERLY RESTRICTED DATA.

TABLE 2. (U) DYNAMIC PRESSURE IMPULSE VERSUS RANGE

CONFIDENTIAL - FORMERLY RESTRICTED DATA

OPERATION/EVENT	SCALED HOB (m)	GROUND RANGE (m)	SCALED GROUND RANGE (m)	S_i	$S_i I_q$ (kPa-sec)	I_q (kPa-sec)	MANNER OF OBTAINING I_q or $S_i I_q$*
Upshot-Knothole, Simon-7	24.7	457	124	0.313	13	41	4
Greenhouse, Easy-2	25.4	457	127	0.284	13.2	46.5	4
		686	190	0.284	14.2	50	4
		915	253	0.264	7.8	27.5	4
Upshot-Knothole, Nancy-2	29.9	457	150	0.378	20	54	4
Upshot-Knothole, Badger-5	30.5	457	152	0.387	17	44	4
Upshot-Knothole, Annie-1	34.4	457	172	0.426	15.5	36.4	2
Tumbler-Snapper, How-7	35.4	503	195	0.455	11	25	4
Tumbler-Snapper, Fox-6	38.8	183	77.6	0.505	26	52	4
		503	213	0.505	12	23.5	4
Teapot, Turk-4	41.1	595	161	0.315	12	36.7	5
		716	193	0.315	9.10	28.9	3
		1030	278	0.315	2.42	7.69	1
		1128	306	0.315	1.78	5.66	1
		1280	345	0.315	0.731	2.32	1**
Teapot, Met-12	41.8	610	210	0.390	16.8	43.0	1
		686	235	0.390	14.7	37.6	1
		762	261	0.390	6.55	16.8	1
		838	287	0.390	5.38	13.8	1
		914	313	0.390	1.37	3.51	1

* 1 - Reference 1 [KT-81-014(R)] Gage and Displacement, except where indicated 2 - BRL Result (Gage)

3 - Average of Our Result (Gage) and BRL Result (Gage) 4 - I_q vs. Displacement Plot for Tanks

5 - Our Gage Result

** Gage Only

TABLE 2. (U) DYNAMIC PRESSURE IMPULSE VERSUS RANGE (Continued)

CONFIDENTIAL - FORMERLY RESTRICTED DATA

OPERATION/EVENT	SCALED HOB (m)	GROUND RANGE (m)	SCALED GROUND RANGE (m)	S_i	$S_i I_q$ (kPa-sec)	I_q (kPa-sec)	MANNER OF OBTAINING I_q or $S_i I_q$ *
Teapot, Apple II-13	47.2	518	161	0.367	18.4	50	3
		625	194	0.367	12.6	34.2	3
		808	250	0.367	5.58	15.2	5
		914	284	0.367	3.78	10.3	1
		1006	311	0.367	2.03	5.54	1
		1128	349	0.367	1.46	3.98	1
		1219	377	0.367	0.936	2.55	1
Teapot, Zucchini-14	47.3	610	189	0.359	8.85	24.6	3
		700	217	0.359	8.78	24.4	3
		794	246	0.359	5.16	14.4	3
Teapot, Hornet-5	56.9	256	159	0.696	17.0	24.5	2
		329	205	0.696	10.8	15.5	2
		460	286	0.696	2.85	4.1	2
Plumbbob, Smoky-15	57.3	457	123	0.324	47.0	145	3
		726	195	0.324	9.23	28.5	1
		841	226	0.324	5.18	16.0	1
		897	241	0.324	4.05	12.5	1
		1038	278	0.324	2.24	6.9	1
		1181	317	0.324	1.22	3.75	1
Teapot, Apple I-8	59.2	527	206	0.460	7.95	17.3	1**
		622	243	0.460	4.35	9.45	3
		808	317	0.460	1.47	3.20	2
		902	352	0.460	0.897	1.95	1
		991	387	0.460	0.552	1.20	1
		1128	440	0.460	0.175	0.38	1

TABLE 2. (U) DYNAMIC PRESSURE IMPULSE VERSUS RANGE (Continued)

CONFIDENTIAL - FORMERLY RESTRICTED DATA

OPERATION/EVENT	SCALED HOB (m)	GROUND RANGE (m)	SCALED GROUND RANGE (m)	S_i	$S_i I_q$ (kPa-sec)	I_q (kPa-sec)	MANNER OF OBTAINING I_q or $S_i I_q$*
Upshot-Knothole, Grable-10	62.4	116	45.3	0.440	39.6	90	2
		174	68.0	0.440	36.5	83	2
		218	85.2	0.440	32.1	73	2
		319	125	0.440	22.9	52	2
		430	168	0.440	13.6	31	2
		736	288	0.440	2.26	5.13	1
		844	330	0.440	1.18	2.69	1
		914	357	0.440	0.62	1.4	2
		1372	536	0.440	0.0440	0.1	2
Teapot, Moth-2	65.0	287	204	0.799	5.39	6.75	1**
		366	260	0.799	2.68	3.35	1**
		411	292	0.799	1.93	2.42	1
		457	325	0.799	1.48	1.85	1
		518	368	0.799	1.08	1.35	1**
Plumbbob, Kepler-9	66.5	762	332	0.513	0.88	1.72	3
Plumbbob, Wilson-4	66.9	305	134	0.506	18.7	37	2
		381	167	0.506	9.4	18.5	2
		518	227	0.506	6.1	12	2
		595	261	0.506	2.1	4.1	2
		671	295	0.506	1.1	2.2	2
Plumbbob, Owens-10	68.3	305	137	0.521	11.9	22.8	3
		457	205	0.521	7.2	13.8	5
		518	232	0.521	5.8	11.2	3
Teapot, Bee-6	73.3	549	264	0.543	4.40	8.10	1
		610	294	0.543	2.26	4.17	1
		701	337	0.543	1.26	2.32	1
		777	374	0.543	1.04	1.91	1

TABLE 2. (U) DYNAMIC PRESSURE IMPULSE VERSUS RANGE (Continued)

CONFIDENTIAL - FORMERLY RESTRICTED DATA

OPERATION/EVENT	SCALED HOB (m)	GROUND RANGE (m)	SCALED GROUND RANGE (m)	S_i	$S_i I_q$ (kPa-sec)	I_q (kPa-sec)	MANNER OF OBTAINING I_q or $S_i I_q$*
Teapot, Post-11	76.6	269	225	0.967	7.7	7.95	3
		320	268	0.967	2.6	2.7	5
		426	357	0.967	1.20	1.25	3
		601	503	0.967	0.29	0.30	5
Plumbbob, Hood-6	103.6	518	117	0.263	5.3	20.2	2
		915	207	0.263	2.84	10.8	2
		1524	345	0.263	1.08	4.1	2
		1829	415	0.263	0.45	1.7	2
Redwing, Yuma-4 †	109	76	133	1.806 †	5.07	2.81	1
		107	187	1.806	2.82	1.56	1
		122	213	1.806	2.60	1.44	1
Teapot, Wasp Prime-9	145	237	152	0.763	6.59	8.63	1
		465	299	0.763	1.39	1.82	1**
		618	397	0.763	0.665	0.871	1**
Plumbbob, Franklin-2	171	243	447	2.164	0.435	0.201	2
Upshot-Knothole, Encore-9	240	756	245	0.366	1.29	3.52	1**
		872	283	0.366	1.10	3.00	1**
		933	303	0.366	1.01	2.75	1**
		1198	389	0.366	0.667	1.82	1**
		1329	431	0.366	0.554	1.51	1**
		1704	553	0.366	0.304	0.830	1**
		1996	648	0.366	0.249	0.680	1**

† This event and the scaling factor in combination are CONFIDENTIAL-FORMERLY RESTRICTED DATA.

TABLE 3. (U) SUMMARY OF DISPLACEMENT DATA FOR TANKS AND HOWITZERS

UNCLASSIFIED

OPERATION/EVENT	SCALED HOB (m)	VEHICLE	ORIEN-TATION	GROUND RANGE (m)	SCALED GROUND RANGE (m)	I_q* (kPa-sec)	DISPLACE-MENT (m)	POINT NO.
U.S. TANKS:								
Upshot-Knothole, Simon-7	24.7	M4A3	FO	457	124	41	6	13
Greenhouse, Easy-2	25.4	M46	SO	457	127	46.5	18	1
		M26	FO	457	127	46.5	6	11
		M26	SO	686	190	50	15	2
		M26	FO	686	190	50	14	12
		M26	SO	915	253	27.5	0.9	3
		M26	RO	686	190	50	16	26
Upshot-Knothole, Nancy-2	29.9	M24	FO	457	150	54	22.9	14
Upshot-Knothole, Badger-5	30.5	M4A3	FO-45°	457	152	44	9	27
Upshot-Knothole, Annie-1	34.4	M24	FO	457	172	36.4	18.3	15
Tumbler-Snapper, How-7	35.4	M4	SO	503	195	25	0.6	4
Tumbler-Snapper, Fox-6	38.8	M46	SO	183	77.6	52	15	5
		M24	FO	503	213	23.5	0.45	16
Teapot, Met-12	41.8	M48	SO	610	210	43	3.45	6
		M48	FO	610	210	43	1.68	17
		M48	FO-45°	610	210	43	4	B

* From Table 2

TABLE 3. (U) SUMMARY OF DISPLACEMENT DATA FOR TANKS AND HOWITZERS (Continued)

UNCLASSIFIED

OPERATION/EVENT	SCALED HOB (m)	VEHICLE	ORIEN-TATION	GROUND RANGE (m)	SCALED GROUND RANGE (m)	I_q* (kPa-sec)	DISPLACE-MENT (m)	POINT NO.
Teapot, Apple II-13	47.2	M24	FO	518	161	50	45.8	18
		M48	SO	625	194	34.2	18.9	7
		M48	FO	625	194	34.2	7	19
		M24	FO	914	284	10.3	0.3	20
		M48	FO-3/4, Left	625	194	34.2	40	C
Plumbbob, Smoky-15	57.3	M48	SO	371	99.6	183**	4.6	8
Upshot-Knothole, Grable-10	62.4	M4A3	SO	174	68.0	83	37.2	9
		M24	FO	174	68.0	83	11.3	21
		M24	FO	218	85.2	73	45	22
		M4A3	SO	319	125	52	32.3	10
		M4A3	RO	319	125	52	40.6	A
Dice Throw	0	M60	FO	177	167	5.75††	0.27	23
		M551	FO	250	236	1.75††	0.051	24
		M551	SO	250	236	1.75††	0.03	25
Self-Propelled Howitzers:								
Upshot-Knothole, Simon-7	24.7	S/P M7 105	FO	229	61.9	76†	46	30
Upshot-Knothole, Badger-5	30.5	S/P M7 105	FO-45°	457	152	40†	18.3	28
			FO-45°	914	305	4.6†	1	29

* From Table
** From Curve Fit (Extrapolated)
† From Fits and SHOB Contours (Results Averaged)
†† From Figure 3.14 of Reference 1

TABLE 3. (U) SUMMARY OF DISPLACEMENT DATA FOR TANKS AND HOWITZERS (Continued)

UNCLASSIFIED

OPERATION/EVENT	SCALED HOB (m)	VEHICLE	ORIEN-TATION	GROUND RANGE (m)	SCALED GROUND RANGE (m)	I_q* (kPa-sec)	DISPLACE-MENT (m)	POINT NO.
Teapot, Turk-4	41.1	T97 S/P 155	FO	716	193	28.9	13.7	32
Teapot, Met-12	41.8	T97 S/P 155	RO	610	210	43.0	15	34
Teapot, Apple II-13	47.2	T97 S/P 155	FO	625	194	34.2	9.6	35
Teapot, Apple I-8	59.2	T97 S/P 155	SO	622	243	9.45	1.5	33
Upshot-Knothole, Grable-10	62.4	S/P M7 105	SO	430	168	31	77	31
Dice Throw	0	M109 S/P 175	FO	226	213	2.6**	0.089	36

* From Table 2
**From Figure 3.14 of Reference 1

TABLE 4. (U) LEAST SQUARES FIT RESULTS
Dynamic Pressure Impulse vs. Displacement and Displacement vs. Dynamic Pressure Impulse

UNCLASSIFIED

VEHICLE (FIGURE NO.)	EVENTS INCLUDED	YIELD RANGE (KT)	N	FIT	$S_{\ell n I_q}$ ($S_{\ell n D}$)	S'_{I_q} (S'_D)	$\sigma_{\ell n I_q, C}$ ($\sigma_{\ell n D, C}$)	$\sigma'_{I_q, C}$ ($\sigma'_{D, C}$)	E_{I_q}(%) [E_D(%)]	m (ℓ)	σ_m (σ_ℓ)	$\sigma_{m/m}$ ($\sigma_{\ell/\ell}$)
M24, M4A3, M48 (1)	Annie-1, Met-12, Apple II-13, Grable-10	14.9 - 28.5	14	$I_q = 24.33D^{0.2354}$; $r = 0.6881$; $r^2 = 0.4735$; $D = 0.005904 I_q^{2.012}$	1.824 (15.60)	2.179 (34.31)	0.3899 (1.140)	0.4261 (1.691)	39.45 (156.6)	0.2354 (2.012)	0.07164 (0.6124)	0.3044 (0.3044)
S/P M-7, 105; T-97, S/P 155 (2)	Simon-7, Badger-5, Turk-4, Met-12, Apple II-13, Apple I-8, Grable-10	14.2 - 43.4	8	$I_q = 7.249D^{0.5262}$; $r = 0.8788$; $r^2 = 0.7723$; $D = 0.09397 I_q^{1.468}$	1.304 (3.636)	1.024 (19.06)	0.4661 (0.7785)	0.4131 (1.782)	35.77 (154.3)	0.5262 (1.468)	0.1166 (.3254)	0.2216 (0.2216)

TABLE 5. (U) LEAST SQUARES FIT RESULTS
Scaled Dynamic Pressure Impulse vs. Scaled Ground Range

CONFIDENTIAL - FORMERLY RESTRICTED DATA

BURST CONDITIONS/ SHOB (Weighted Average) (m) *(FIGURE NO.)*	EVENTS INCLUDED	YIELD RANGE (KT)	N	FIT RANGE OF x DATA (Fit x_{min} or x_{max})	R^2	$S_{\ell nS_iI_q}$	$S'_{S_iI_q}$	$\sigma_{\ell nS_iI_q,C}$	$\sigma'_{S_iI_q,C}$	$E_{S_iI_q}$ (%)
Light Dust, 34.28 *(3)*	Simon-7 Easy-2 Nancy-2 Badger-5 Annie-1 How-7 Fox-6 Turk-4	11.1 - 46.7	15	$\ell nS_iI_q = 2.517+0.009525x-0.00005135x^2$ $77.6 \leq x \leq 345$ $(x_{max} = 92.75)$	0.9378	0.8590	0.9180	0.2676	0.2766	24.74
Heavy Dust, 41.8 *(4)*	Met-12	22.0	5	$\ell nS_iI_q = -5.159+0.07913x-0.0001960x^2$ $210 \leq x \leq 313$ $(x_{max} = 201.9)$	0.9608	0.1578	0.1678	0.2809	0.2897	18.32
Moderate-Heavy Dust, 47.23 *(5)*	Apple II-13 Zucchini-14	28.2 - 28.5	10	$\ell nS_iI_q = 4.857-0.01228x-0.000001992x^2$ $161 \leq x \leq 377$ (-----------)	0.9815	0.1550	0.1396	0.1488	0.1412	11.81
Light Dust, 57.98 *(6)*	Hornet-5 Smoky-15 Apple I-8	3.61 - 43.71	15	$\ell nS_iI_q = 6.040-0.02038x+0.000007122x^2$ $123 \leq x \leq 440$ $(x_{min} = 1430)$	0.9871	0.3694	0.3963	0.1754	0.1817	16.25

TABLE 5. (U) LEAST SQUARES FIT RESULTS (Continued)
Scaled Dynamic Pressure Impulse vs. Scaled Ground Range

CONFIDENTIAL - FORMERLY RESTRICTED DATA

BURST CONDITIONS/ SHOB (Weighted Average) (m) (FIGURE NO.)	EVENTS INCLUDED	YIELD RANGE (KT)	N	FIT RANGE OF x DATA (Fit x_{min} or x_{max})	R^2	$S_{\ell nS_iI_q}$	$S'_{S_iI_q}$	$\sigma_{\ell nS_iI_q},C$	$\sigma'_{S_iI_q},C$	$E_{S_iI_q}$ (%)
Light Dust, 64.69 (7)	Grable-10 Moth-2 Kepler-9 Wilson-4 Owens-10	2.39 - 14.9	23	$\ell nS_iI_q = 4.388-0.01131x-0.000004960x^2$ $45.3 \le x \le 536$ (-----------)	0.9777	1.279	1.368	0.2529	0.2615	24.38
Moderate-Heavy Dust, 74.95 (8)	Bee-6 Post-11	1.45 - 7.76	8	ℓnS_iI_q 3.496-0.02438x+0.00001805x^2 $225 \le x \le 503$ (x_{min} = 675.5)	0.9751	0.1745	0.1613	0.1868	0.1796	14.20
Near-Ideal, 122.5 (9)	Hood-6 Yuma-4 * Wasp Prime-9 Franklin-2	0.138 - 74.1	11	$\ell nS_iI_q = 2.688-0.007646x-0.0000007894x^2$ $117 \le x \le 447$ (------------)	0.9737	0.2556	0.3102	0.1788	0.1969	16.79
Near-Ideal, 240 (10)	Encore-9	26.0	7	$\ell nS_iI_q = 1.776-0.006752x+0.000002785x^2$ $245 \le x \le 648$ (x_{min} = 1217)	0.9952	0.01169	0.01126	0.05405	0.05307	4.01

* This event and the SHOB in combination are CONFIDENTIAL - FORMERLY RESTRICTED DATA

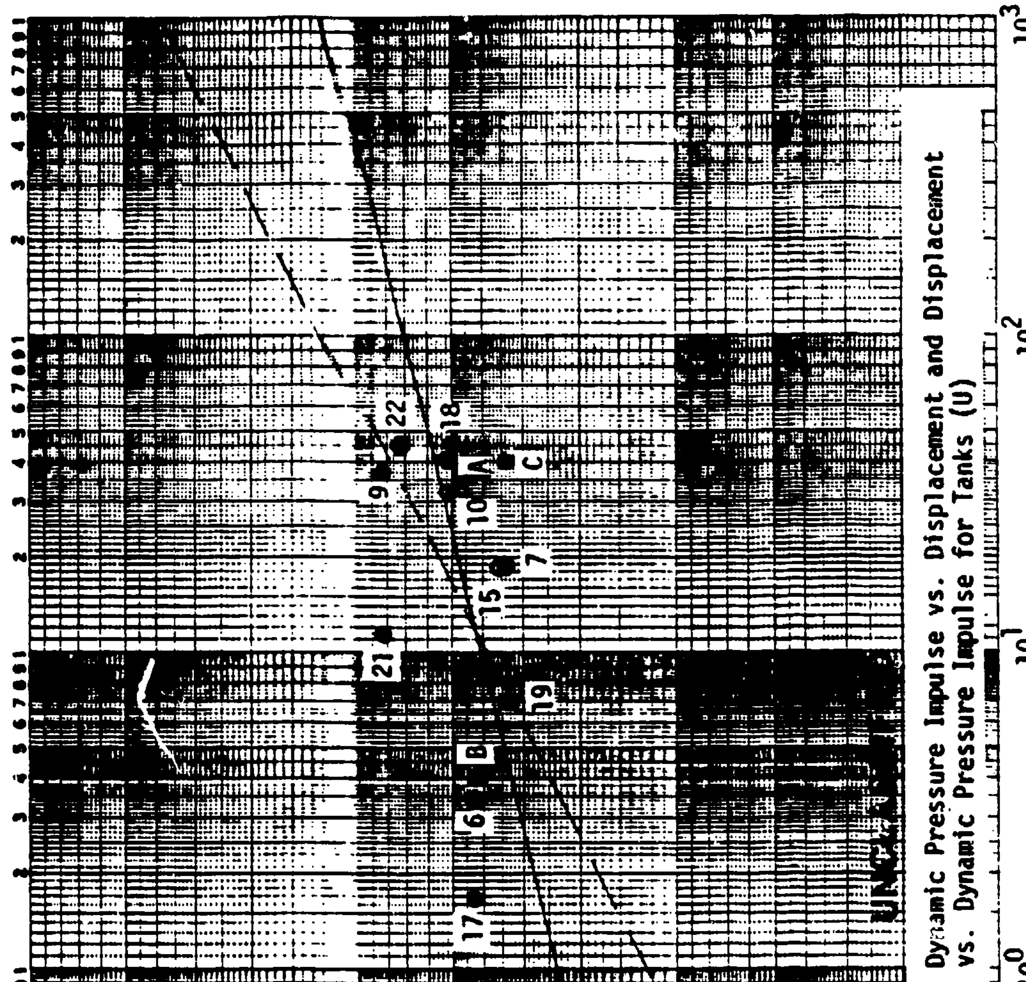

FIGURE 1 (U) Dynamic Pressure Impulse vs. Displacement and Displacement vs. Dynamic Pressure Impulse for Tanks (U)

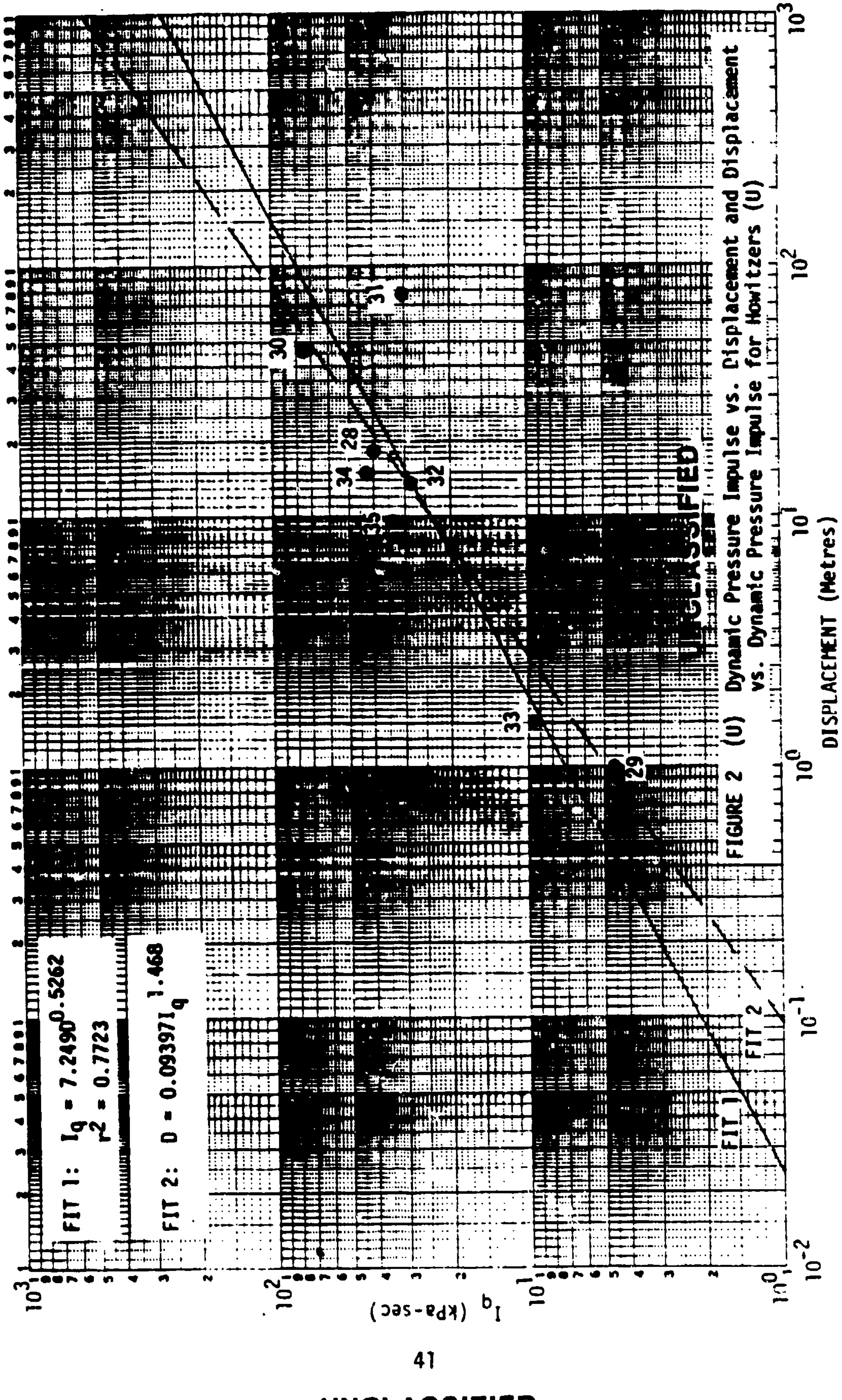

FIGURE 2 (U) Dynamic Pressure Impulse vs. Displacement and Displacement vs. Dynamic Pressure Impulse for Howitzers (U)

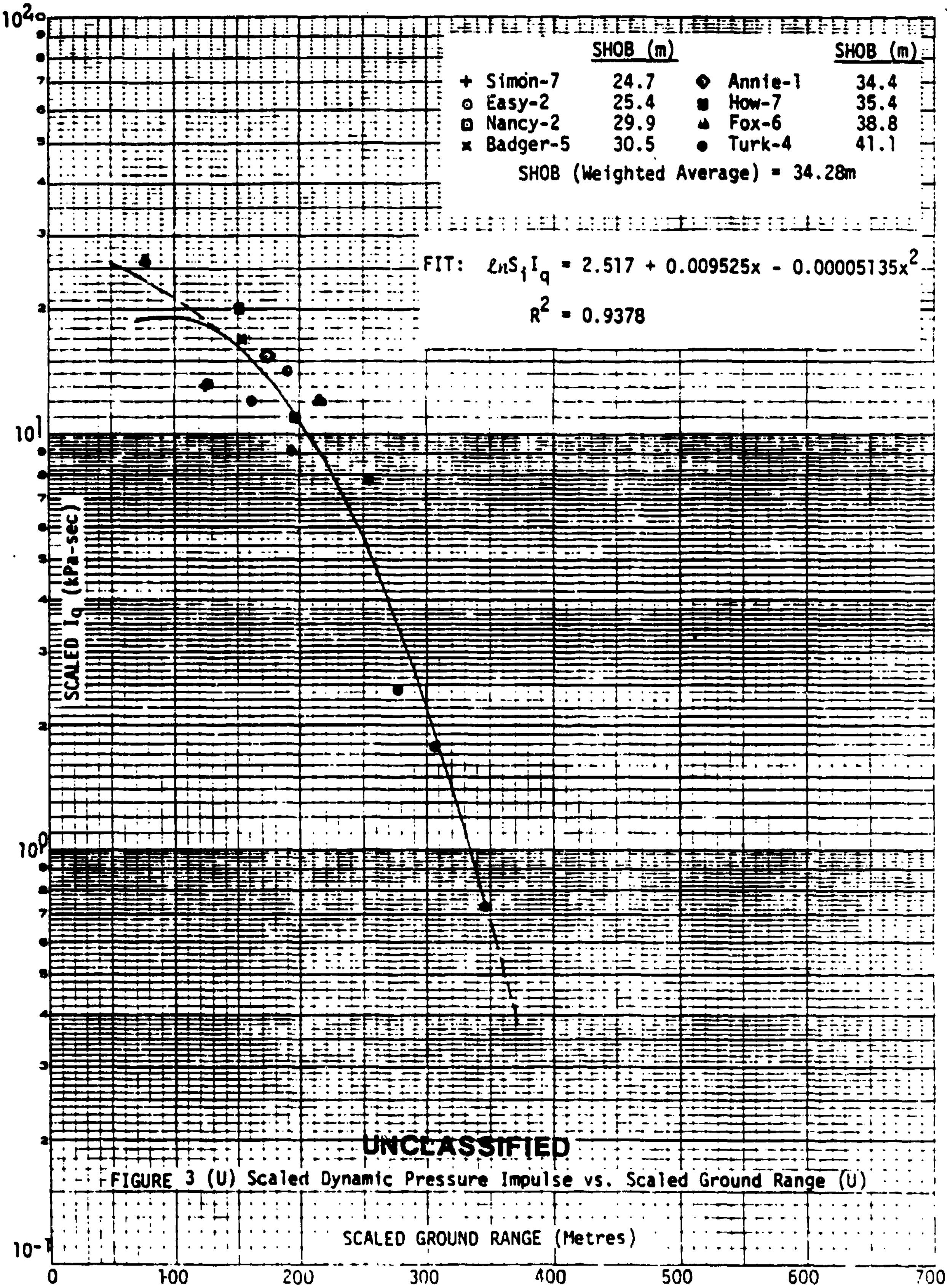

UNCLASSIFIED

FIGURE 3 (U) Scaled Dynamic Pressure Impulse vs. Scaled Ground Range (U)

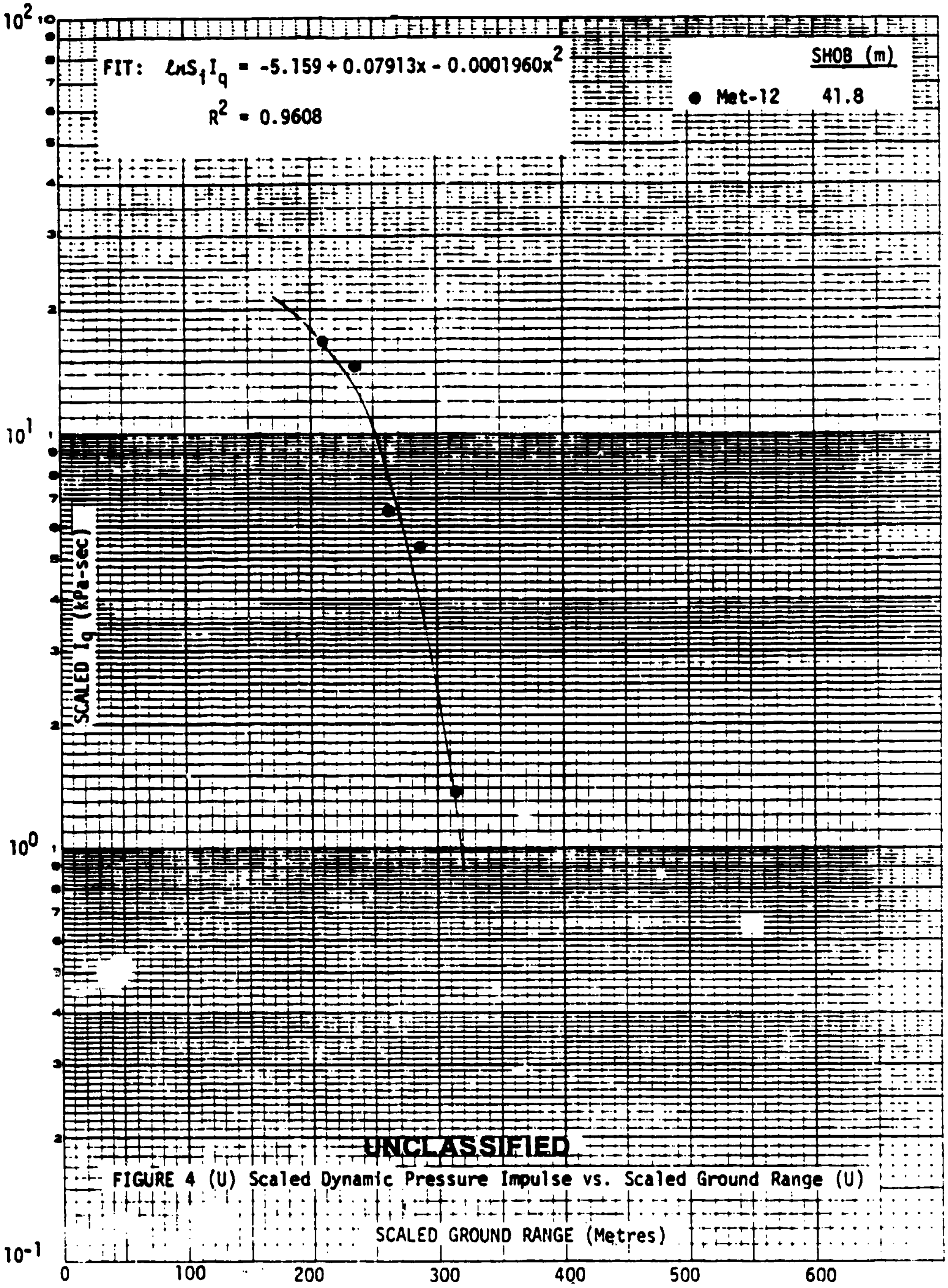

UNCLASSIFIED

FIGURE 4 (U) Scaled Dynamic Pressure Impulse vs. Scaled Ground Range (U)

UNCLASSIFIED

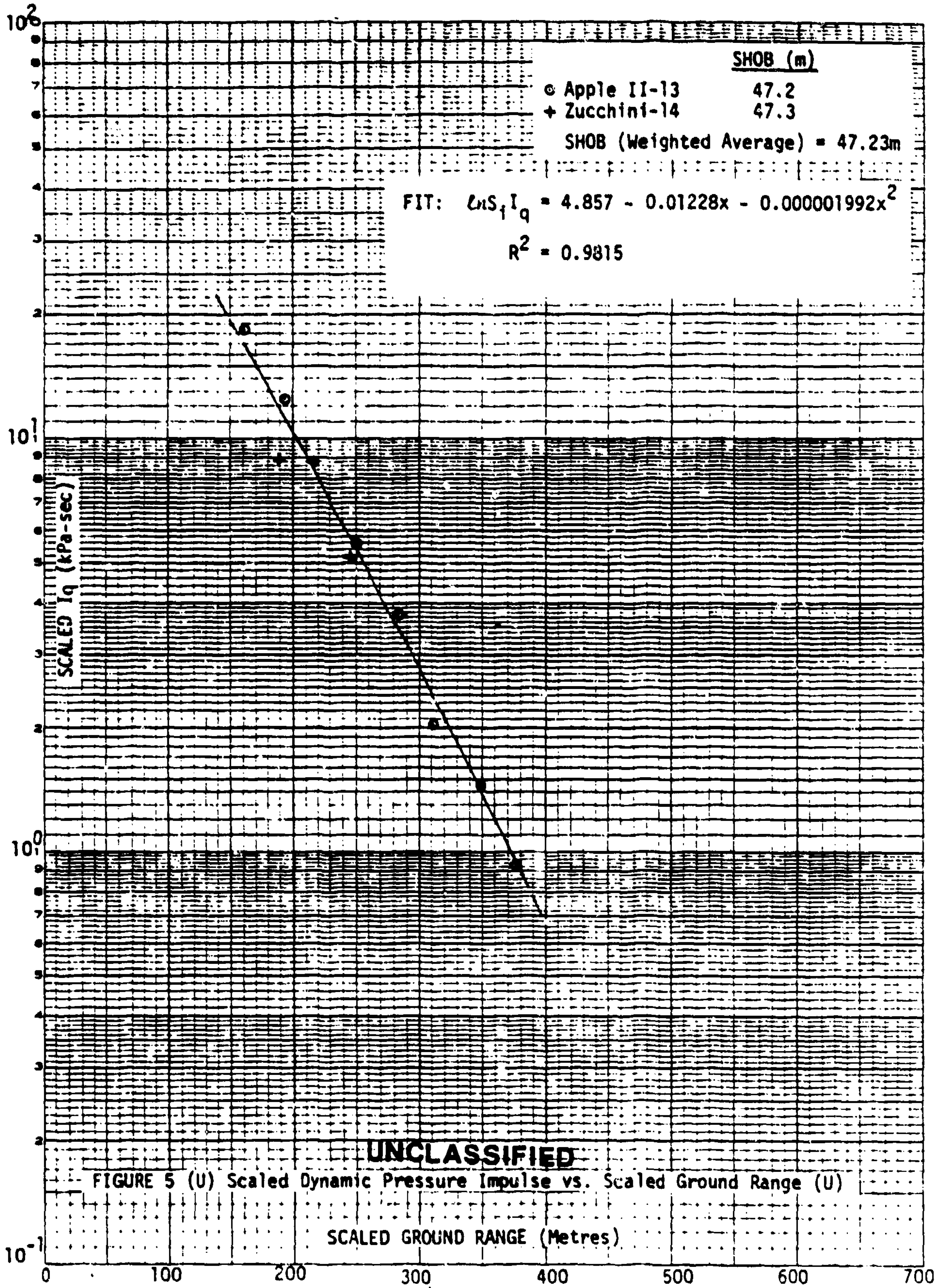

UNCLASSIFIED

FIGURE 5 (U) Scaled Dynamic Pressure Impulse vs. Scaled Ground Range (U)

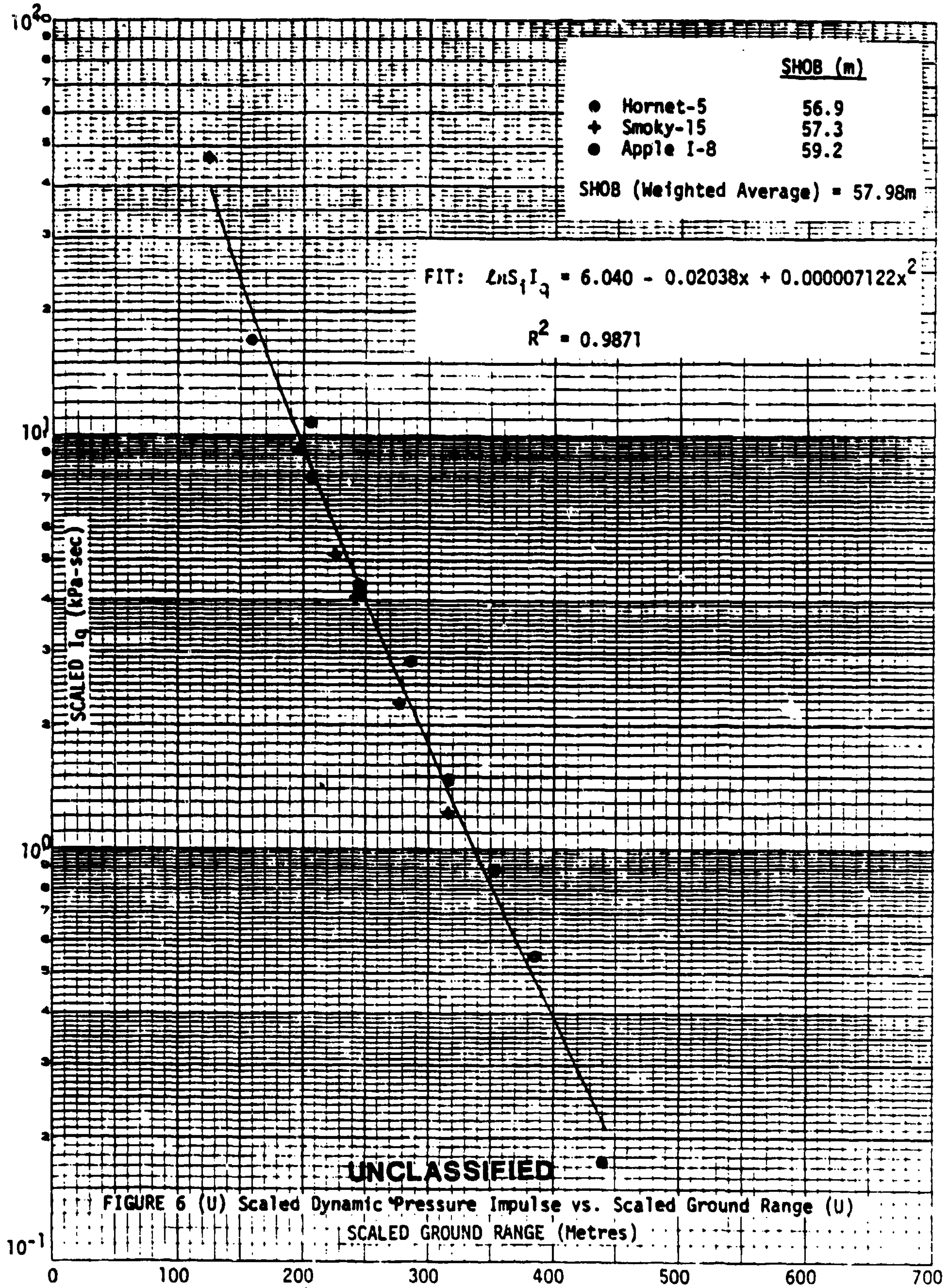

FIGURE 6 (U) Scaled Dynamic Pressure Impulse vs. Scaled Ground Range (U)

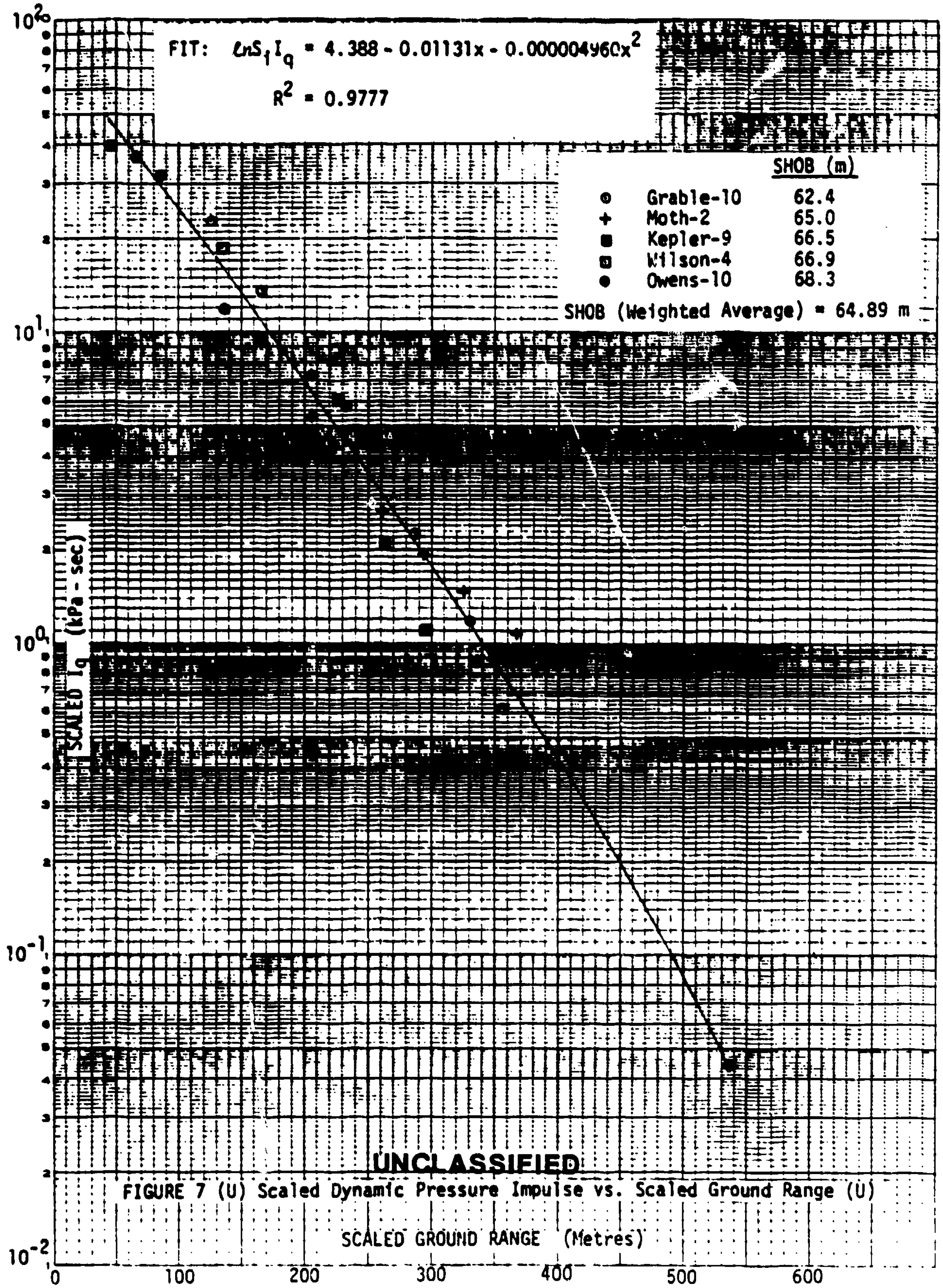

FIGURE 7 (U) Scaled Dynamic Pressure Impulse vs. Scaled Ground Range (U)

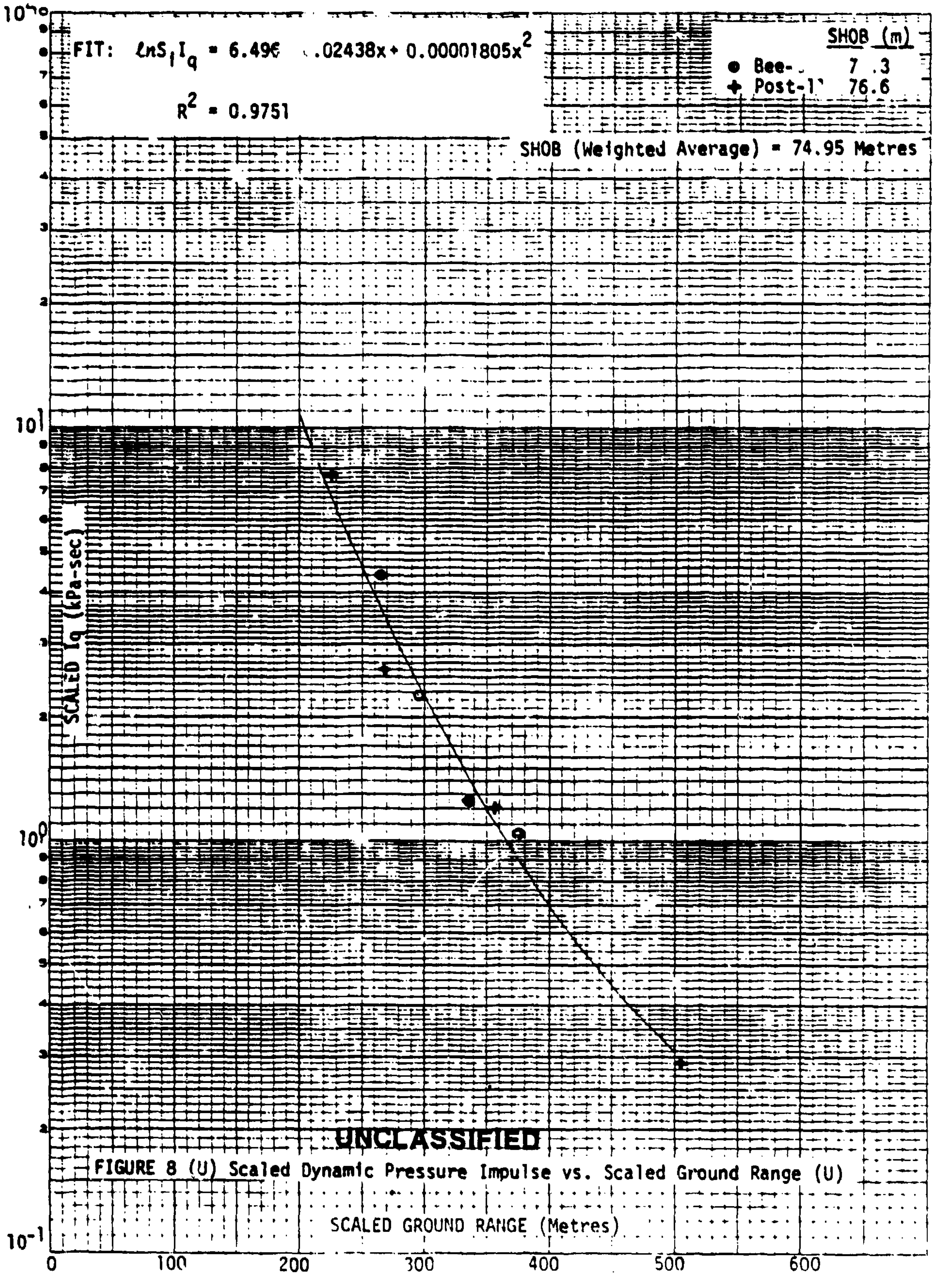

FIGURE 8 (U) Scaled Dynamic Pressure Impulse vs. Scaled Ground Range (U)

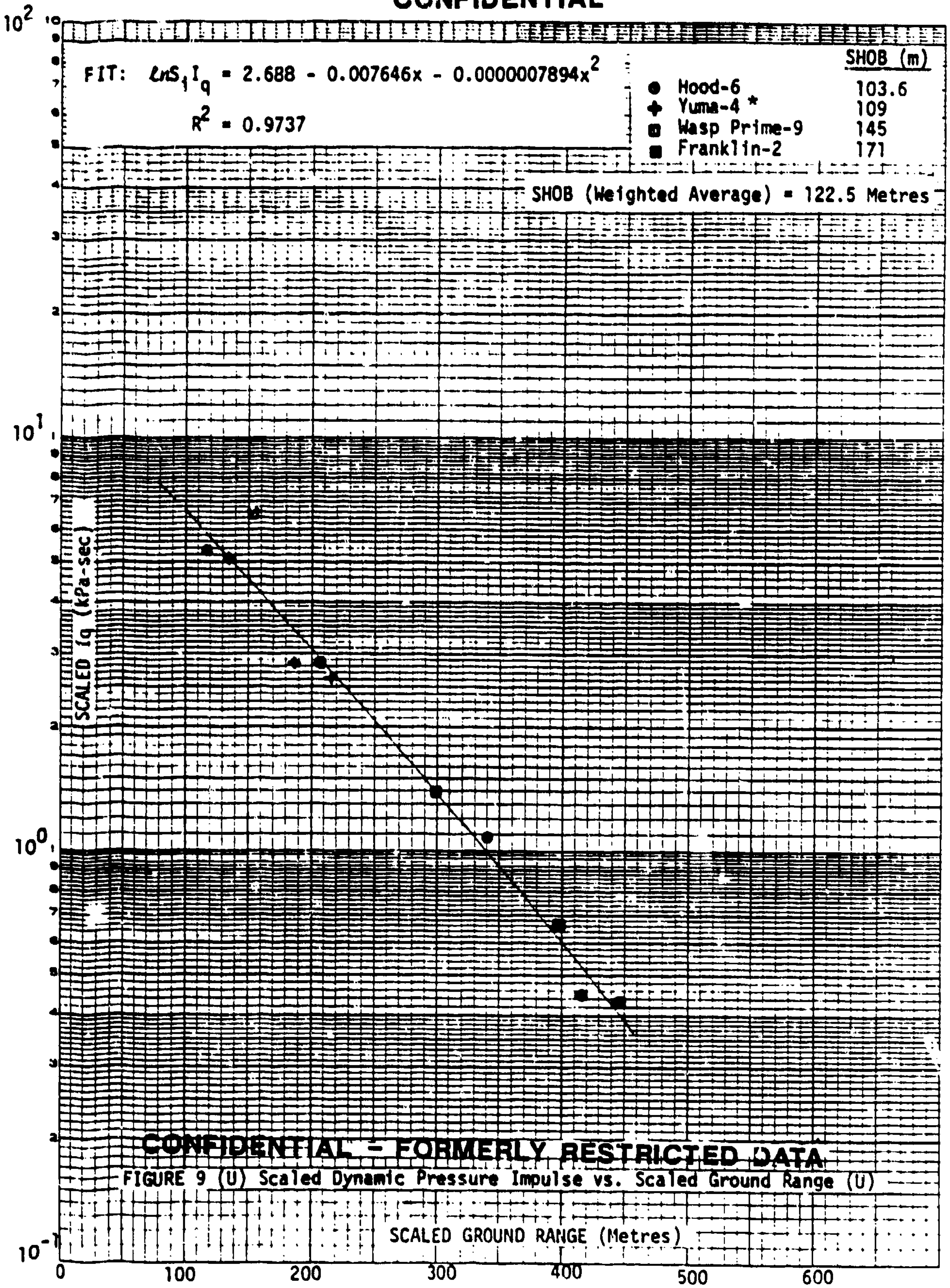

CONFIDENTIAL - FORMERLY RESTRICTED DATA

FIGURE 9 (U) Scaled Dynamic Pressure Impulse vs. Scaled Ground Range (U)

*This event and the SHOB in combination are CONFIDENTIAL - FORMERLY RESTRICTED DATA

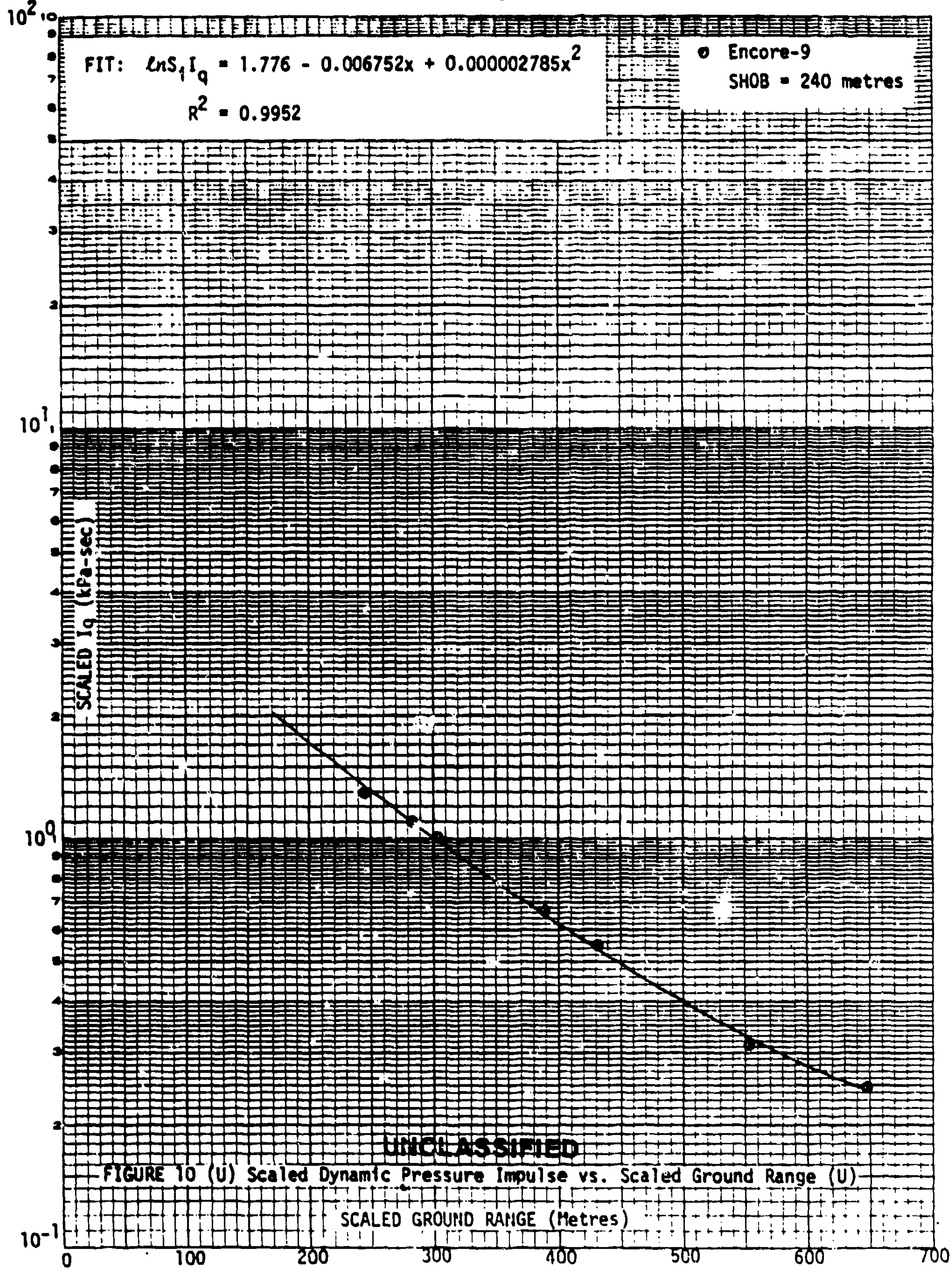

UNCLASSIFIED

FIGURE 10 (U) Scaled Dynamic Pressure Impulse vs. Scaled Ground Range (U)

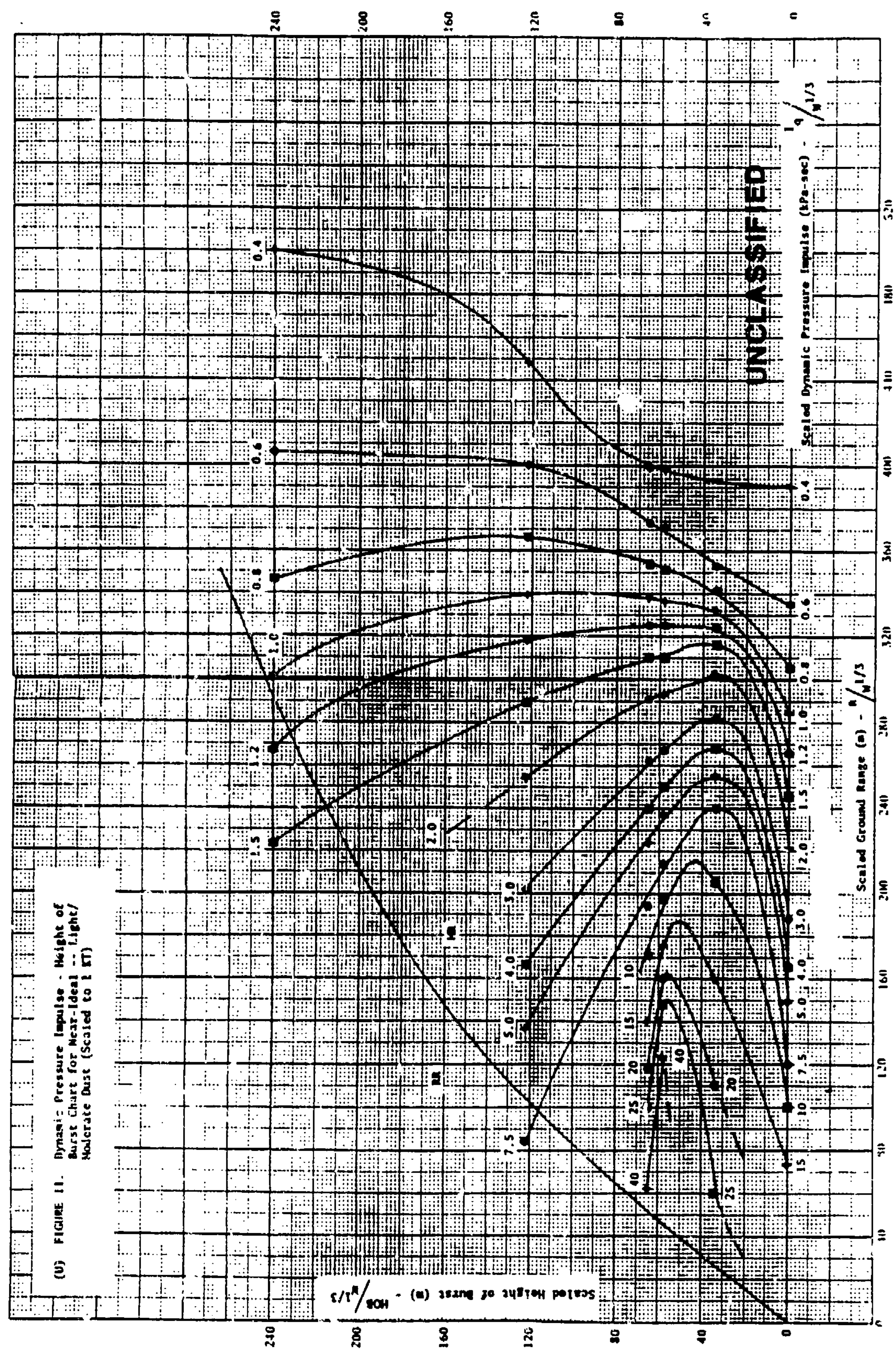

(U) FIGURE 11. Dynamic Pressure Impulse - Height of Burst Chart for Near-Ideal -- Light/ Moderate Dust (Scaled to 1 KT)

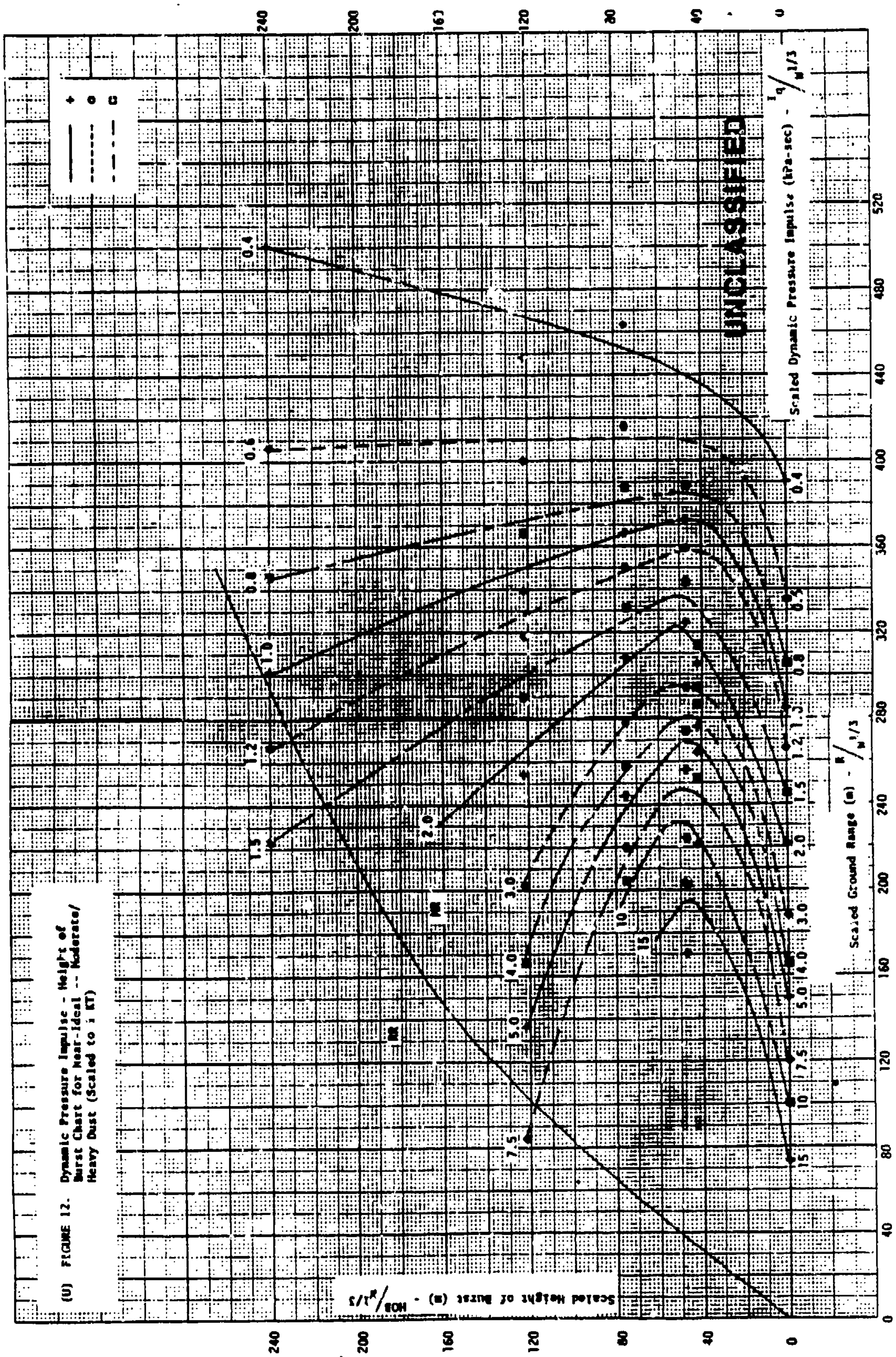

(U) FIGURE 12. Dynamic Pressure Impulse - Height of Burst Chart for Near-Ideal -- Moderate/Heavy Dust (Scaled to 1 KT)

THIS PAGE IS INTENTIONALLY LEFT BLANK.

DISTRIBUTION LIST

(This List Is Unclassified)

DEPARTMENT OF DEFENSE

DEF RSCH & ENGRG
ATTN: STRAT & SPACE SYS(OS)
ATTN: STRAT & THTR NUC FOR/F VAJDA

DEFENSE INTELLIGENCE AGENCY
ATTN: RTS-2A (TECH LIB)
ATTN: RTS-2B

DEFENSE NUCLEAR AGENCY
ATTN: SPAS C GALLOWAY
ATTN: SPAS D MUNNINGHOFF
ATTN: SPAS G ULLRICH
ATTN: SPAS R ROHR
4 CYS ATTN: TITL

DEFENSE TECHNICAL INFORMATION CENTER
2 CYS ATTN: DD

FIELD COMMAND DEFENSE NUCLEAR AGENCY
ATTN: FCTT
ATTN: FCTT W SUMMA
ATTN: FCTXE

JOINT STRAT TGT PLANNING STAFF
ATTN: JKCS
ATTN: JPEP
ATTN: JPTM

DEPARTMENT OF THE ARMY

HARRY DIAMOND LABORATORIES
ATTN: SCHLD-NW-P
ATTN: SLCIS-IM-TL (81100) (TECH LIB)

U S ARMY BALLISTIC RESEARCH LAB
ATTN: SLCBR-SS-T (TECH LIB)

U S ARMY CORPS OF ENGINEERS
ATTN: DAEN-ECE-T

U S ARMY ENGINEER CTR & FT BELVOIR
ATTN: TECHNICAL LIBRARY

U S ARMY ENGINEER DIV HUNTSVILLE
ATTN: HNDED-SY

U S ARMY ENGR WATERWAYS EXPER STATION
ATTN: E JACKSON, WESSS-O
ATTN: J JACKSON, WESSD
ATTN: J ZELASKO, WESSD-R

U S ARMY NUCLEAR & CHEMICAL AGENCY
ATTN: LIBRARY
ATTN: MONA-NU MR LONG

U S ARMY STRATEGIC DEFENSE COMMAND
ATTN: DASD-H-L
ATTN: DASD-H-SAV R DUDNEY

DEPARTMENT OF THE NAVY

NAVAL RESEARCH LABORATORY
ATTN: CODE 2627 (TECH LIB)
ATTN: CODE 4040 D BOOK
ATTN: CODE 4040 J BORIS

NAVAL SURFACE WEAPONS CENTER
ATTN: CODE R44 H GLAZ
ATTN: CODE X211 (TECH LIB)

NAVAL SURFACE WEAPONS CENTER
ATTN: TECH LIBRARY & INFO SVCS BR

DEPARTMENT OF THE AIR FORCE

AIR FORCE CTR FOR STUDIES & ANALYSIS
ATTN: AFCSA/SAMI (R GRIFFIN)

AIR FORCE WEAPONS LABORATORY, NTAAB
ATTN: NTED-A
ATTN: SUL

BALLISTIC MISSILE OFFICE/DAA
ATTN: ENSN
ATTN: MYEB D GAGE

STRATEGIC AIR COMMAND/NRI-STINFO
ATTN: NRI/STINFO

DEPARTMENT OF ENERGY

LOS ALAMOS NATIONAL LABORATORY
ATTN: C F KELLER
ATTN: M T SANDFORD
ATTN: R WHITAKER

SANDIA NATIONAL LABORATORIES
ATTN: DIV 7111 J W REED
ATTN: J R BANNISTER 7111
ATTN: ORG 7112 A CHABAI

OTHER GOVERNMENT

CENTRAL INTELLIGENCE AGENCY
ATTN: OSWR/NED

DEPARTMENT OF DEFENSE CONTRACTORS

AEROSPACE CORP
ATTN: H MIRELS
ATTN: LIBRARY ACQUISITION

APPLIED RESEARCH ASSOCIATES, INC
ATTN: N HIGGINS

APPLIED RESEARCH ASSOCIATES, INC
ATTN: D PIEPENBURG

BOEING CO
ATTN: G R BURWELL

CALIFORNIA RESEARCH & TECHNOLOGY, INC
ATTN: K KREYENHAGEN
ATTN: LIBRARY

CALIFORNIA RESEARCH & TECHNOLOGY, INC
ATTN: F SAUER

CARPENTER RESEARCH CORP
ATTN: H J CARPENTER

DENVER COLORADO SEMINARY UNIVERSITY OF
ATTN: J WISOTSKI

H & H CONSULTANTS, INC
ATTN: J HALTIWANGER
ATTN: W HALL

H-TECH LABS, INC
ATTN: B HARTENBAUM

KAMAN SCIENCES CORP
ATTN: R RUETENIK

KAMAN TEMPO
ATTN: DASIAC
2 CYS ATTN: E BRYANT
2 CYS ATTN: F ALLEN

KAMAN TEMPO
ATTN: DASIAC

MCDONNELL DOUGLAS CORP
ATTN: H HERDMAN
ATTN: R HALPRIN

NEW MEXICO, UNIVERSITY OF
ATTN: J KOVARNA

PACIFIC-SIERRA RESEARCH CORP
ATTN: H BRODE, CHAIRMAN SAGE

PACIFIC-SIERRA RESEARCH CORP
ATTN: D GORMLEY

PACIFICA TECHNOLOGY
ATTN: R ALLEN
ATTN: TECH LIBRARY

PHYSICS INTERNATIONAL CO
ATTN: H W WAMPLER

R & D ASSOCIATES
ATTN: A KUHL
ATTN: T MAZZOLA
ATTN: TECHNICAL INFORMATION CENTER

R & D ASSOCIATES
ATTN: A POLK
ATTN: B WEBSTER

R & D ASSOCIATES
ATTN: G GANONG

RAND CORP
ATTN: B BENNETT

S-CUBED
ATTN: B PYATT
ATTN: C DISMUKES
ATTN: J BARTHEL
ATTN: LIBRARY

S-CUBED
ATTN: C NEEDHAM

SCIENCE APPLICATIONS INTL CORP
ATTN: H WILSON
ATTN: R SCHLAUG
ATTN: TECHNICAL LIBRARY

SCIENCE APPLICATIONS INTL CORP
ATTN: J COCKAYNE
ATTN: W LAYSON

SCIENCE APPLICATIONS INTL CORP
ATTN: G BINNINGER

SRI INTERNATIONAL
ATTN: J COLTON

TELEDYNE BROWN ENGINEERING
ATTN: D ORMOND
ATTN: F LEOPARD

TRW ELECTRONICS & DEFENSE SECTOR
ATTN: A ZIMMERMAN
ATTN: M SEIZEW
ATTN: TECH INFO CTR, DOC ACQ.

TRW ELECTRONICS & DEFENSE SECTOR
ATTN: N GUILES
ATTN: N LIPNER

WEIDLINGER ASSOC, CONSULTING ENGRG
ATTN: I SANDLER

Defense Special Weapons Agency
6801 Telegraph Road
Alexandria, Virginia 22310-3398

TRC 13 April 1998

MEMORANDUM TO DEFENSE TECHNICAL INFORMATION CENTER
ATTN: OCQ/MR BILL BUSH

The following reports have been reviewed by the Defense Special Weapons Agency Security Office:

~~DNA-4622F, AD-C015969, DTL-78,1304~~ 321 Completed
DNA-5056F, AD-C021924, DTL-80,0808
DNA-5826F, AD-C040572, DTL-87,0355 C FRD
DNA-5826F-SUP, AD-C041417, DTL-871167 C FRD

The Security Office has **declassified** all of the listed reports. Further, distribution statement **"A"** applies to all of the reports.

Ardith Jarrett
ARDITH JARRETT
Chief, Technical Resource Center

Completed
15 May 2000
B.W.